# 論文 / 著書情報
# Article / Book Information

| | |
|---|---|
| 題目(和文) | ポリビニルアルコールとボロノフェニルアラニンを基盤とする薬物送達システムの応用と機能改変 |
| Title(English) | Application and Functional Modification of Drug Delivery Systems based on Poly(vinyl alcohol) and Boronophenylalanine |
| 著者(和文) | 小成田翔 |
| Author(English) | Kakeru Konarita |
| 出典(和文) | 学位:博士(工学),<br>学位授与機関:東京科学大学,<br>報告番号:甲第357号,<br>授与年月日:2025年3月26日,<br>学位の種別:課程博士,<br>審査員:西山 伸宏,三浦 裕,中村 浩之,田中 克典,門之園 哲哉,曽根 正人 |
| Citation(English) | Degree:Doctor (Engineering),<br>Conferring organization: Institute of Science Tokyo,<br>Report number:甲第357号,<br>Conferred date:2025/3/26,<br>Degree Type:Course doctor,<br>Examiner:,,,,, |
| 学位種別(和文) | 博士論文 |
| Category(English) | Doctoral Thesis |
| 種別(和文) | 要約 |
| Type(English) | Outline |

2025 Doctoral thesis

# Application and Functional Modification of Drug Delivery Systems based on Poly(vinyl alcohol) and Boronophenylalanine


Department of Life Science and Technology

Name: Kakeru Konarita

Academic Adviser: Prof. Nobuhiro Nishiyama

# Contents



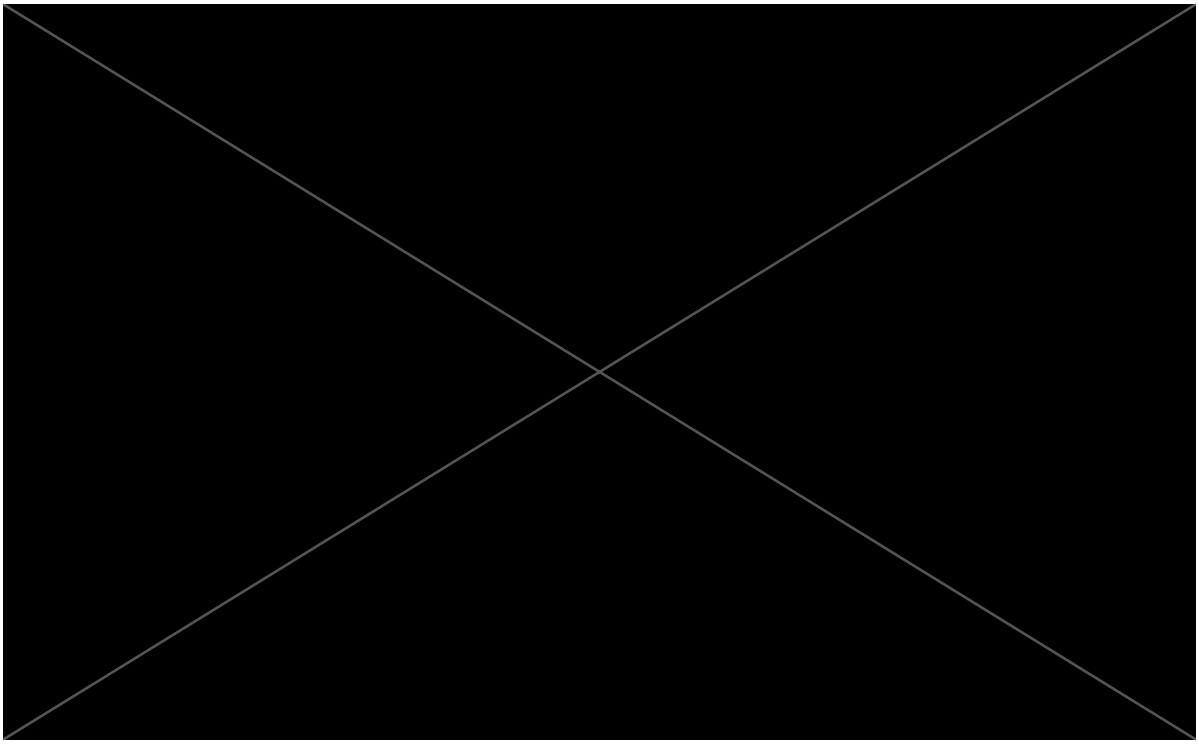

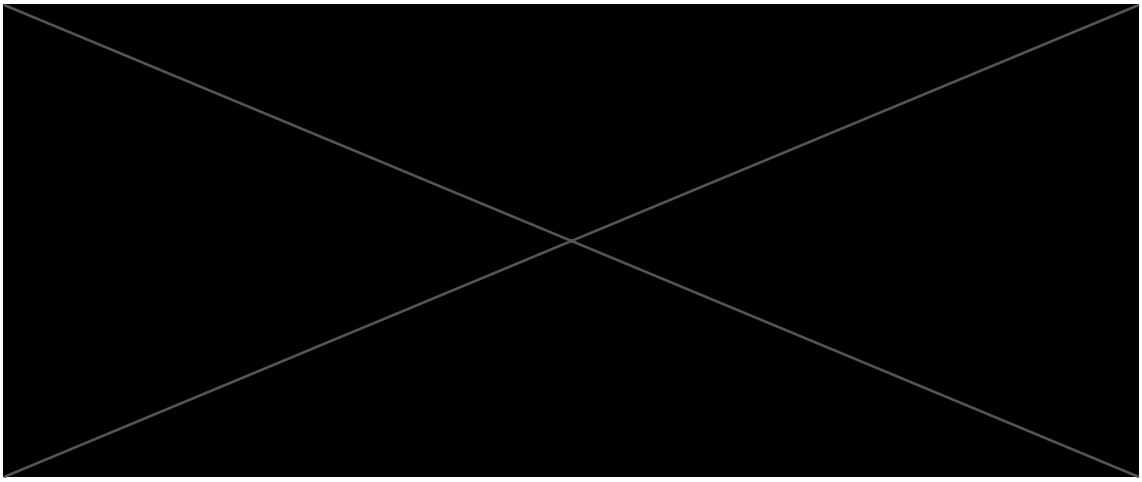



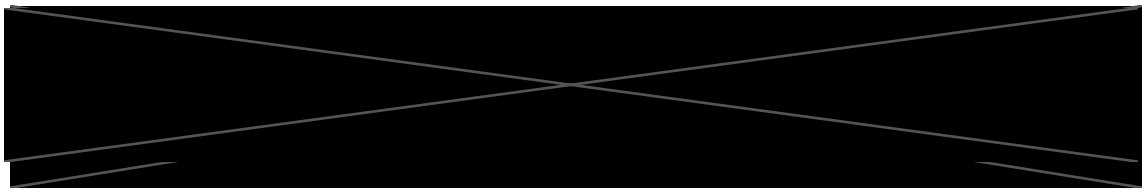

# ABBREVIATIONS

A

- Active pharmaceutical ingredient (API)
- Aspartate aminotransferase (AST)

B

- Blood-brain barrier (BBB)
- Blood urea nitrogen (BUN)
- Boron neutron capture therapy (BNCT)
- Boronophenylalanine (BPA)
- $Na_2B_{12}H_{11}SH$ (BSH)
- 2-aminobicyclo(2,2,1)heptane-2-carboxylic acid (BCH)

C

- Chimeric antigen receptor T-cell (CAR-T)
- Creatinine (CRE)

D

- Deoxyribonucleic acid (DNA)
- Drug delivery system (DDS)
- D-4-boronophenylalanine (D-BPA)
- 5-(diethylamino)-2-((methylimino)methyl)phenol (DAHMI)

E

- Enhanced permeability and retention effect (EPR effect)

G

- Good Laboratory Practice (GLP)
- Good Manufacturing Practice (GMP)
- Glutamate oxaloacetate transaminase (GOT)

H

- Human epidermal growth factor receptor 2 (HER2)
- Human papillomavirus (HPV)

I

- Immune checkpoint inhibitor (ICI)

- In vivo imaging system (IVIS)

L

- Large neutral Amino acid Transporter 1 (LAT1)
- Linear energy transfer (LET)
- L-4-boronophenylalanine (L-BPA)

M

- N-(carbonyl-methoxypolyethylene glycol 2000)-1,2-distearoyl- Coated with sn-glycerol-3-phosphoethanolamine sodium salt (MPEG-DSPE)
- Malignant pleural mesothelioma (MPM)

N

- Noncommunicable diseases (NCDs)

P

- Pharmaceuticals and Medical Devices Agency (PMDA)
- Poly(vinyl alcohol) (PVA)
- Polyethylene glycol (PEG)

R

- Reactive oxygen species (ROS)

S

- Stereotactic ablative radiotherapy (SABR)

T

- Tumor-to-Normal tissue ratio (T/N ratios)

V

- Vascular endothelial growth factor (VEGF)

# CHAPTER 1

# (General Introduction)

## 1.1 Cancer and the treatments

Cancer, malignant tumors are cells or tissues in which genetic abnormalities have been caused by internal or external factors, which cells continue to proliferate without being subject to organizational control within the body, causing invasion and metastasis into surrounding tissues. Cancer remains a significant challenge in the 21st century, posing a serious societal, public health, and economic burden. It accounts for nearly one in six deaths globally (16.8%) and over one-fifth (22.8%) of deaths caused by noncommunicable diseases (NCDs) [1]. The disease is responsible for 30.3% of premature deaths from NCDs in individuals aged 30–69 and ranks among the top three causes of death in this age group across 177 of 183 countries [2]. Beyond limiting life expectancy, cancer imposes considerable societal and economic costs, which differ by cancer type, region, and gender [3]. A recent study highlighted the devastating impact of cancer mortality among women, revealing that approximately one million children became maternal orphans in 2020 due to their mothers' cancer-related deaths. Nearly half of these cases were linked to breast or cervical cancer [4]. Against this background, it is thought that the demand for cancer treatment will continue to rise worldwide. Modern cancer treatment methods are roughly divided into 4 types: surgical treatment, chemotherapy, radiotherapy, and immune therapy, and an overview of these is briefly explained below.

### 1.1.1 Surgical treatment

Surgical treatment involves surgically removing the focal site of the tumor. If it is resectable, this is the first treatment method, and unless there are undetected micrometastases, there is a high possibility of a complete cure. However, this treatment is highly invasive, requiring a long recovery time after surgery, and depending on the area removed, organ and body functions may be impaired [5].

In recent years, in order to minimize this disadvantage, intraperitoneal surgery using an endoscope (small camera) and reduction surgery that minimizes the area to be removed have become more popular [6].

## 1.1.2 Chemotherapy

Chemotherapy is a treatment in which anticancer drugs are administered into the bloodstream or other parts of the body to kill cancer cells [7]. Basically, chemotherapy is effective by inhibiting biological activities such as DNA synthesis and suppressing cell proliferation. Cancer cells divide at a faster rate than normal cells, making anticancer drugs highly effective, and this therapy is often used. In addition, because the drugs are administered systemically, they are effective against small metastases that are easily missed, and can be used when tumors are present in areas that are not resectable. However, anticancer drugs are often effective against normal tissues, resulting in serious side effects such as vomiting, hair loss, fatigue, numbness, and damage to the liver, kidneys, and hematopoietic organs [8]. To overcome this drawback, technologies have been developed in order to target only cancer tissue or the biomolecules necessary to maintain the vital activities of cancer cancer cells. Drug delivery system (DDS) is a technology that targets only cancer tissues [9]. DDS is a technology oriented to maximize the effects of drugs by controlling the ideal pharmacokinetics of drugs in the body. This technology aims to deliver the drug where it is needed, in the right amount, and at the right time. For delivery to tumors, DDS technology has long been widely known for its microenvironmental properties. Tumor tissue produces angiogenic factors, such as vascular endothelial growth factor (VEGF), to secure a large amount of nutrients, causing the formation of new blood vessels around cancer cells [10]. Unlike normal vascular endothelial cells, there are relatively large gaps of about 200 nm in diameter between vascular endothelial cells in cancer tissue. Therefore, macromolecules with a hydrodynamic diameter of approximately 100–200 nm can selectively accumulate in tumor tissue. In addition, since the lymphatic system, which is an excretory pathway, is underdeveloped in tumor tissue, excretion from tissue fluid through lymphatic vessels is inhibited, and it is known that macromolecules have a relatively high retention property because it is above the threshold of glomerular filtration (<10 nm)[11]. The increased vascular permeability of macromolecular drugs in tumor tissues and their long-term retention in tissues with an underdeveloped lymphatic system are referred to as the Enhanced Permeability and Retention Effect (EPR)[12] (**Figure 1.1.2.1**).

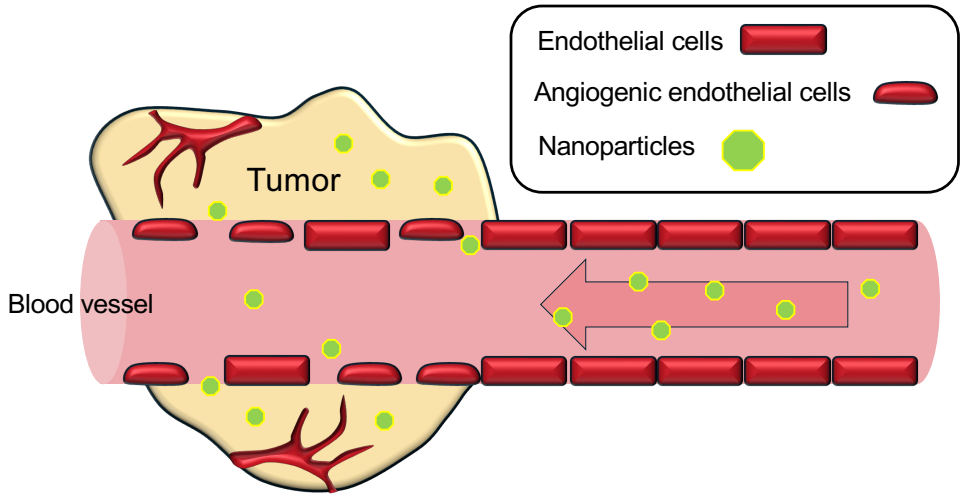


**Figure 1.1.2.1 Schematic illustration of enhanced permeability and retention (EPR) effect of nanoparticles in tumors**

In addition, as a DDS formulation that utilizes the EPR effect (particle size 70~100)[13], Doxil® has been used clinically. Doxil® has the formulation where doxorubicin hydrochloride (an anticancer drug) is encapsulated in liposomes and the surface is coated with a water-soluble polymer, *N*-[carbonyl-(methoxypolyethylene glycol)-2000]-1,2-distearoyl-*sn*-glycerol-3-phosphoethanolamine (MPEG-DSPE) (**Figure 1.1.2.2**).

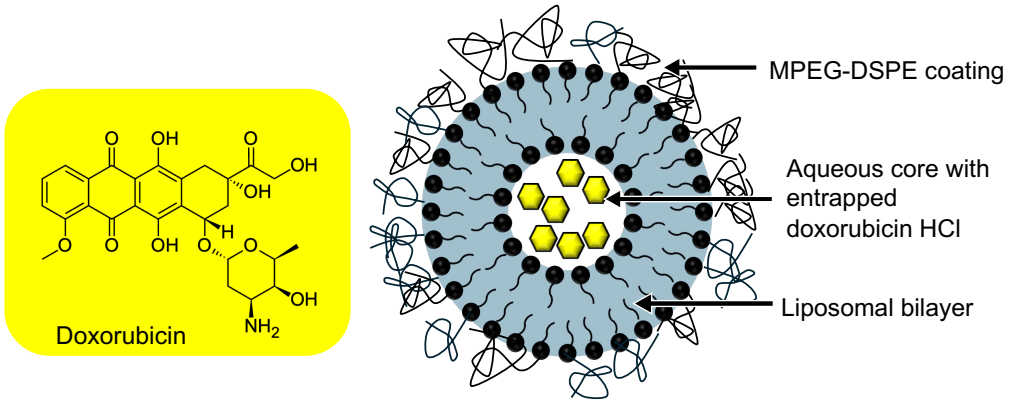


**Figure 1.1.2.2 The structure of Doxil® (Pegylated Liposomal Doxorubicin)**

Sufficient blood retention of the drug carrier is required to utilize the EPR effect, which requires appropriate particle size and minimization of the foreign body processing mechanism of the organism. Specifically, since molecules smaller than 10

nm are renally excreted from the blood and those larger than 200 nm are captured by macrophages in the spleen and Kupffer cells in the liver, it is necessary to have a particle size in that range, and to avoid interaction with blood components such as serum albumin and complement, coating with biocompatible materials such as polyethylene glycol (PEG) is necessary to cover the drug carrier. Such a DDS strategy is then called passive targeting.

In contrast, a DDS strategy that delivers a drug to cancer cells through active interaction, for example, by using molecules that specifically bind to the target, such as antibodies that bind to receptors specifically expressed on cancer cells, is called active targeting. An example of a drug that utilizes active targeting is L-p-boronophenylalanine, which is the subject of this study.

## 1.1.3 Radiotherapy

Radiation therapy achieves therapeutic effects by irradiating tumor tissue with ionizing radiation such as X-rays, gamma rays, electron beams, and heavy particle beams, damaging the DNA of cancer cells and killing them. Radiotherapy is usually applied to cancers which surgery is not possible. Also, it has no effect on areas other than the irradiated area, so it has less impact on the whole body than general chemotherapy [5]. However, the cell-killing effect appears in normal tissue in a straight line of the irradiated area toward cancer, and the total radiation dose that can be tolerated in radiation therapy is limited, so multiple or recurrent cancers are generally not suitable for radiation therapy.

Radiosensitivity also depends on the type and condition of the tumor. In conventional X-ray therapy, cells in the G2 and M phases are more sensitive [14], while hypoxic cells are less sensitive [15, 16]. This is because X-rays, γ-rays, and β-ray indirectly cause DNA damage mainly by producing reactive oxygen species (ROS) at the irradiated site. In contrast, radiation with high linear energy transfer (LET) per unit of radiation trajectory (heavy particle beams), such as carbon beams, mainly cause direct DNA damage and are therefore relatively effective even in hypoxic cells that are resistant to X-rays and γ-rays (**Figure 1.1.3.1**). Boron neutron capture therapy (BNCT), the subject of this study, is also classified as a radiation therapy (heavy particle beam). The alpha particles and Li nuclei produced by the nuclear reaction between thermal

neutrons and $^{10}B$ utilized in BNCT have a high LET and the cell killing effect of these particles exceeds that of carbon beams.

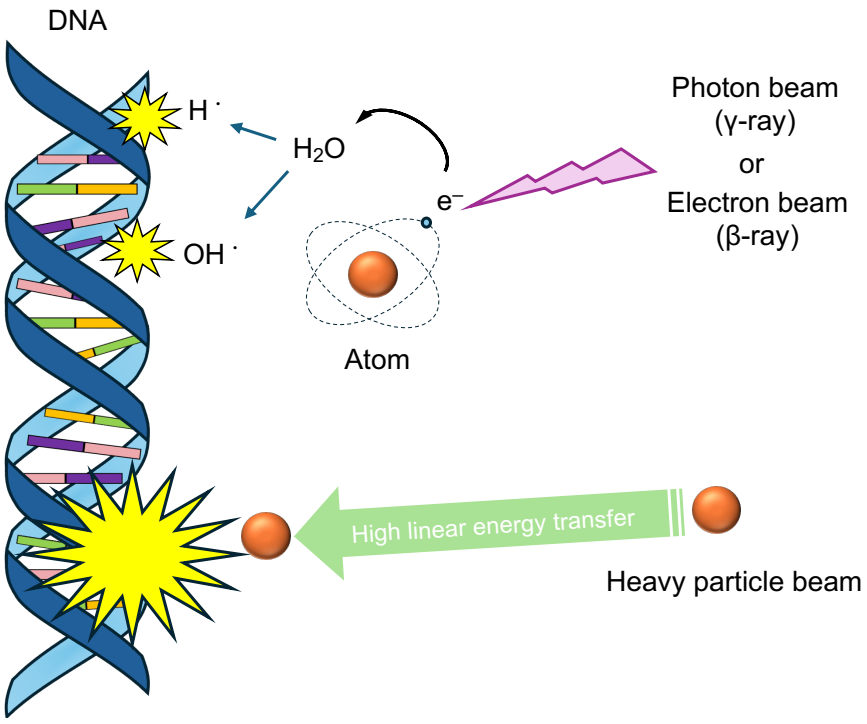


**Figure 1.1.3.1 The mechanism of Radiation Therapy**.

## 1.1.4 Immunotherapy

Immunotherapy is a transformative approach in cancer treatment that leverages the body's immune system to identify and eliminate cancer cells. Unlike conventional therapies, such as chemotherapy or radiation, immunotherapy aims to enhance the immune system's natural capacity to combat cancer while sparing healthy cells. The major modalities of immunotherapy include immune checkpoint inhibitors, cancer vaccines, adoptive cell transfer, and monoclonal antibodies. Immune checkpoint inhibitors (e.g., anti-PD-1, anti-CTLA-4) work by releasing the brakes on immune cells, enabling them to attack cancer more effectively. For instance, pembrolizumab, an anti-PD-1 agent, has shown remarkable efficacy in melanoma and non-small cell lung cancer [17]. Adoptive cell transfer therapies, such as chimeric antigen receptor T-cell (CAR-T) therapy, involve engineering

patients' T cells to target tumor antigens, yielding promising results in hematologic malignancies like B-cell lymphomas [18]. Cancer vaccines, both therapeutic and prophylactic, stimulate immune responses against cancer-specific antigens. For example, the human papillomavirus (HPV) vaccine effectively prevents cervical cancers linked to high-risk human papillomavirus strains [19]. Monoclonal antibodies, including trastuzumab for human epidermal growth factor receptor 2 (HER2)-positive breast cancer, target specific cancer proteins and may also recruit immune cells for tumor destruction. Despite its success, immunotherapy faces challenges, such as limited efficacy in certain cancers, immune-related adverse events, and high costs. Research continues to focus on overcoming these barriers by combining immunotherapies with other treatments and identifying predictive biomarkers [20]. By harnessing the power of the immune system, immunotherapy represents a paradigm shift in oncology, offering hope for improved survival and quality of life for cancer patients.

## 1.1.5 Boron Neutron Capture Therapy

Boron neutron capture therapy (BNCT) is a new cancer treatment modality that utilizes the nuclear fusion reaction that occurs between thermal neutron beams and boron ($^{10}$B) [21-23]. When $^{10}$B absorbs neutrons, it splits into $^{4}$He nuclei (α particles) and $^{7}$Li nuclei, and these particles with high LET directly damage cell DNA and induce cell death (**Figure 1.1.5.1**).

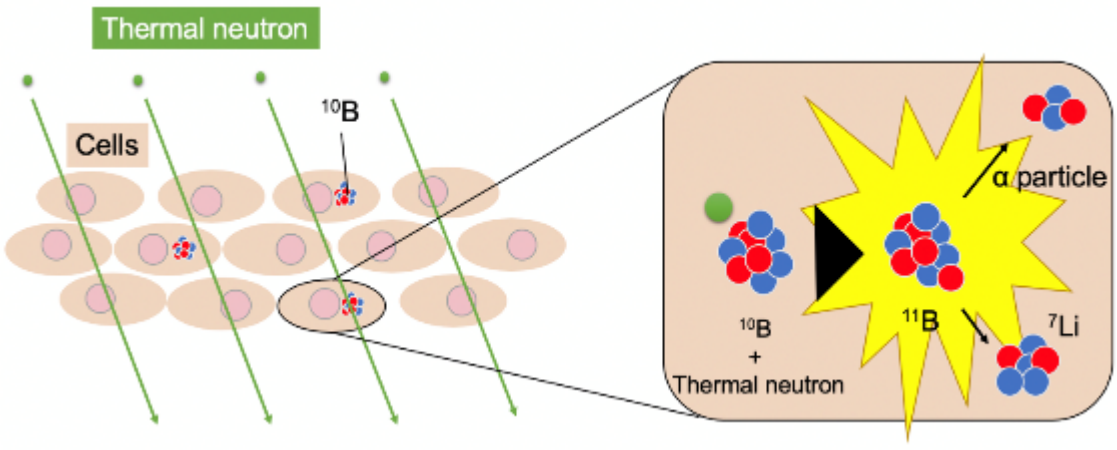


**Figure 1.1.5.1 The principle of BNCT**.

Thermal neutrons are captured by various atomic nuclei existing in living organisms ($^{1}H$, $^{16}O$, $^{14}N$, and $^{12}C$), but $^{10}B$ has a greatly higher probability of capturing neutrons (cross section capture value), and its value is 2000 times larger than that of $^{14}N$, which has the largest neutron capture cross-section among biological atoms (**Table 1.1.5.1**). In addition, the α particles and $^{7}Li$ atomic nuclei generated by the reaction between neutrons and $^{10}B$ have a range of 9-10 μm and 4-5 μm, respectively, which is comparable to the cell diameter, so they selectively kill cancer cells and tissues that contain enough $^{10}B$. So this treatment need boron agents that selectively accumulate to cancer tissue.

**Table 1.1.5.1 Cross section capture values**[24].

| | Reaction | Cross section capture values [*barn] |
|---|---|---|
| $^{1}H$ | $^{1}H$ (n, γ) $^{2}H$ | 0.322 |
| $^{12}C$ | $^{12}C$ (n, γ) $^{13}C$ | 0.0032 |
| $^{16}O$ | $^{16}O$ (n, γ) $^{17}O$ | 0.00018 |
| $^{14}N$ | $^{14}N$ (n, p) $^{14}C$ | 1.82 |
| $^{10}B$ | $^{10}B$ (n, α) $^{7}Li$ | 242 |
| | $^{10}B$ (n, α, γ) $^{7}Li$ | 3595 |

*barn = $10^{-24}$ $cm^2$

To introduce the history of BNCT, the idea of BNCT itself was proposed by American physicist Locher in 1936 [25]. The world's first actual application to cancer treatment was for 10 years starting in 1951, at the Brookhaven National Laboratory and the Massachusetts Institute of Technology's nuclear reactors, for malignant brain tumors [26]. However, the treatment results showed that the average survival time was less than 6 months, and its effectiveness was not proven. The reasons for this failure include the poor cancer-selective accumulation of boron compounds and the low quality of the neutron beam at that time.

Later, in 1968, Hatanaka et al. performed BNCT on patients with malignant brain tumors using the then newly developed boron compound $Na_2B_{12}H_{11}SH$ (commonly known as BSH), and a dramatic therapeutic effect was obtained (see section on boron agents) [27]. Since then, BSH-BNCT has been performed on more than 200

brain tumor patients, but due to the presence of tumors of various malignancies and patient backgrounds, it was not possible to draw a conclusion regarding the usefulness of the treatment effect for specific pathological conditions. Then, in 1987, the world's first successful BNCT for malignant melanoma was achieved using the boron drug L-4-boronophenylalanine (L-BPA), which selectively accumulates in cancer [28]. Its success was certainly supported by the extensive basic research on BPA that had been conducted up to that point. And this success became decisive for the subsequent development of BPA-BNCT (see the section on boron drugs below for details).

## 1.1.5.1 Boron agent

Many boron-containing compounds have been studied so far, but in this section, I will focus on two representative boron compounds that have been used in clinical research, BSH and BPA, and provide a slightly more detailed explanation.

### 1.1.5.1.1 $Na_2B_{12}H_{11}SH$ (BSH)

$Na_2B_{12}H_{11}SH$ (BSH) (**Figure.1.1.5.1.1**) was developed through joint research by Hatanaka and Soloway et al. [29] [10], and among the various boron drugs being developed at the time, it was the first to demonstrate high BNCT therapeutic efficacy for malignant brain tumors [27]. BSH has 12 $^{10}B$ atoms per molecule, so it has excellent $^{10}B$ transport properties and is a highly water-soluble compound. In a normal brain, the blood-brain barrier (BBB) prevents all but a few compounds from penetrating into the brain tissue, but in malignant brain tumors, the BBB is broken, so BSH penetrates and stays only in the tumor tissue. It is thought that this may produce a large difference in $^{10}B$ concentration between the tumor site and the normal brain. However, it does not have the property of being actively taken up by targeting specific molecules in cancer cells.

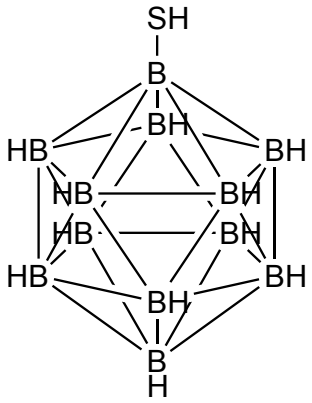


**Figure 1.1.5.1.1 The chemical structure of BSH** [7]

### 1.1.5.1.2 L-4-Boronophenylalanine (L-BPA)

The history of L-4-Boronophenylalanine (L-BPA) begins with its discovery in 1982 by Mishima et al. At that time, Yutaka Mishima tried to treat malignant melanoma, which is an X-ray-resistant skin cancer, by BNCT. And he paid attention to an analogue of tyrosine (a precursor of melanin pigment), L-4-boronophenylalanine, which has boric acid residue at the p-position of the essential alpha amino acid L-phenylalanine. Then he started clinical research of BNCT about L-BPA as specific boron compound for malignant melanoma [28]. (**Figure 1.1.5.1.2.1**).

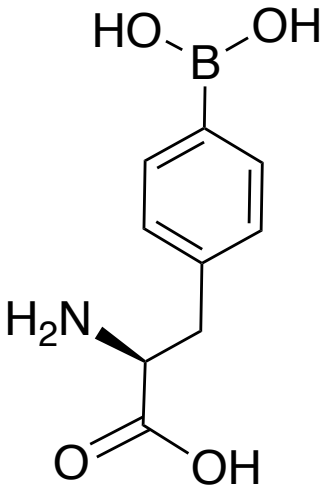


**Figure 1.1.5.1.2.1 The chemical structure of L-BPA**

As a result, a large difference was observed in the uptake between malignant melanoma cells and normal cells, and subsequent research revealed that it is taken up not only by malignant melanoma but also by a wide variety of cancers. Further research revealed that BPA has the property of being taken up through the Large neutral Amino acid Transporter 1 (LAT1), which is upregulated in many cancer cells[30, 31]. The world's first clinical use of L-BPA was in 1987 in BNCT of malignant melanoma patients performed by Mishima et al. In addition, for malignant brain tumors, it was used in BNCT of patients with recurrent malignant glioma at the Kyoto University Reactor (KUR), which was conducted in February 1994, which is seven months earlier than BNCT held at Brookhaven National Laboratory in the United States. From this point, L-BPA is the drug that has undergone the most clinical research and trials to date.

On the other hand, L-BPA has three types of structural isomers: o-isomer (L-2-BPA), m-isomer (L-3-BPA), and p-isomer (L-4-BPA), depending on the position on the benzene ring where the boric acid residue is bonded. Hiratsuka et al. conducted a distribution study using these three structural isomers in a Syrian hamster Greene's melanoma cell transplant model, and found that the p-isomer (position 4) showed a higher intratumor accumulation than other isomers[32]. For this reason, the p-isomer (L-4-BPA) is used in current clinical research and clinical trials. However, a recent study have been reported that L-3-BPA accumulates in tumors to the same extent as that of L-4-BPA [33].

Furthermore, the accumulation of L-BPA in cancer depends on the level of LAT1 expression in cancer cells, and individual differences in the level of LAT1 expression in a patient's cancer tissue usually correlates to the differences in the therapeutic effect of BPA-BNCT. Therefore, companion diagnostics that detect tumor accumulation of L-BPA before treatment are important. In this regard, a non-invasive real-time diagnosis, Positron-Emission-Tomography (PET) has been thought to be eligible for this purpose, and PET agents has been developed. Specifically, 4-borono-2-[$^{18}$F]-fluoro-L-phenylalanine ($^{18}$F-L-BPA), which is labeled at the o-position of L-BPA with fluorine ($^{18}$F, PET nuclide), is planned to be used for actual treatment in the future[34-36](**Figure 1.1.5.1.2.2**). It has also been reported that F-L-BPA and L-BPA exhibit similar pharmacokinetics [37].

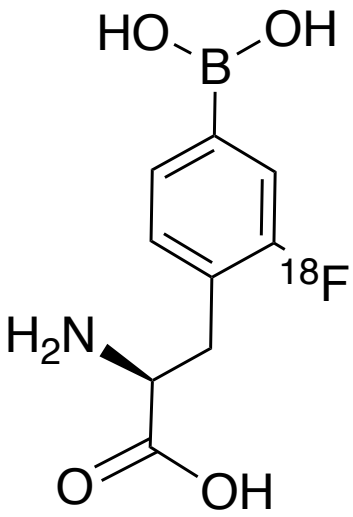


**Figure 1.1.5.1.2.2 The chemical structure of $^{18}$F-L-BPA**

## 1.1.5.2 Problem and challenges in BNCT with L-BPA

### 1.1.5.2.1 Actual L-BPA dosage form and administration method in clinical practice

L-BPA is intended to be administered intravenously and should be in an aqueous solution. L-BPA, which is a zwitterionic ion, has a zero charge at physiological pH (7.4), so its solubility at physiological pH is extremely low. To address this problem, Yoshino et al. improved the water solubility of L-BPA under physiological conditions by complexing with D-fructose via boronic acid ester (Fructose-BPA, **Figure 1.1.5.2.1.1**) [38] [17].

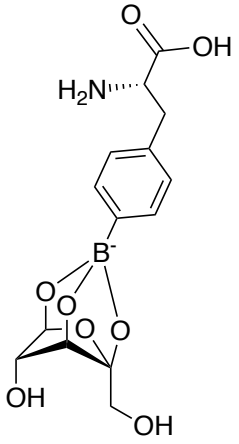


**Figure 1.1.5.2.1.1 The structure of fructose-BPA.**

However, the D-fructose solution of BPA causes a structural change in BPA within 2-3 days due to the Maillard reaction originating from the amino group and carbonyl group. Currently, D-sorbitol, compound the carbonyl group of D-fructose is Reduced, is used to solubilize L-BPA (sorbitol-BPA, **Figure 1.1.5.2.1.2**). In 2020, Stella Pharma Corporation received regulatory approval for sorbitol-L-BPA under the name "STEBORONINE®"[39].

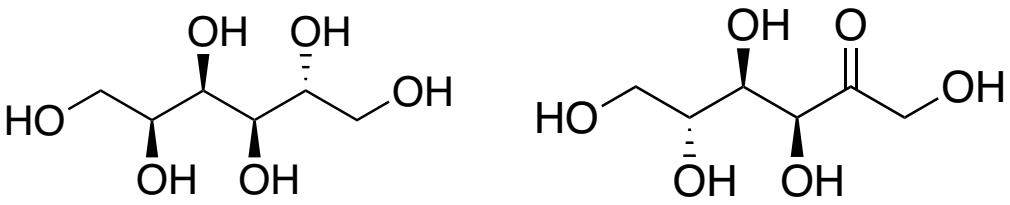


**Figure 1.1.5.2.1.2 The chemical structures of D-sorbitol and D-fructose.**

The actual administration amount of STEBORONINE® is intended to be 500mg BPA/kg to bring the intratumoral boron concentration to 20 ppm or more during neutron irradiation. Specifically, STEBORONINE® is intravenously infused 200 mg/kg/h ×2 h before irradiation by infusion, and 100 mg/kg/h x 1 h from the start to the end of irradiation [39].

### 1.1.5.3 PVA-BPA

The reason why the continues administration method is adopted for sorbitol-BPA is due to the properties of L-BPA and antiport mechanism of LAT1. LAT1 is a sodium-independent neutral amino acid transporter that transport large neutral amino acids such as tyrosine that exist outside the cell, and LAT1 needs exchange of intracellular amino acids when LAT1 transport amino acids extracellular cell into cytosol. Hence, if the extracellular BPA concentration decreases, L-BPA will be exchanged with extracellular amino acids and excreted [40] (**Figure 1.1.5.3.1 A**). Thus, when administration of L-BPA to the blood is interrupted, the L-BPA concentration in the blood decreases due to renal excretion, and L-BPA accumulated in cancer cells is rapidly exchanged and excreted.

Hence, in order to maintain the intratumoral boron concentration sufficiently high during the irradiation time of 30-60 minutes, continuous administration of L-BPA

during irradiation as described above is essential. Further, with the development of neutron irradiation technology, the types of cancers to which BNCT can be applied will become more diverse, including cancers that require longer irradiation times than conventional BNCT (described in introduction of chapter 2). As the more irradiation time, it needs more administration of boron compound, meaning the risk of adverse events derives from overdose. Also, during neutron beam irradiation, only the patient is allowed to enter the treatment room [41], so there remain issues such as being unable to respond immediately to accidents such as an IV needle falling out, or sudden changes in the patient's physical condition. For that reasons, there has been a need to maintain high intratumoral boron concentrations without continuous administration.

In response to this demand, Takahiro Nomoto and his colleagues have developed a method for binding L-BPA to poly(vinyl alcohol) (PVA), a biocompatible and water-soluble polyol-based polymer, via boronic acid ester. It is generally known that polymer compounds cannot permeate cell membranes and are therefore taken into cells by endocytosis. Hence, they hypothesized that if a BPA-bound polymer is taken up by endocytosis, its distribution to the cytoplasm is delayed by passing through endosomes and lysosomes, suppressing the extracellular release of BPA from the cytoplasm by LAT1 (**Figure 1.1.5.3.1 B, C, and D**). This attempt was successful, and PVA and L-BPA actually form a complex, termed PVA-BPA, through boronic acid ester by simple mixing in aqueous solution (Figure 1.1.5.3.1 bottom), and PVA increased the cellular uptake of L-BPA, showing high therapeutic effect enough to completely cure of cancer [42].

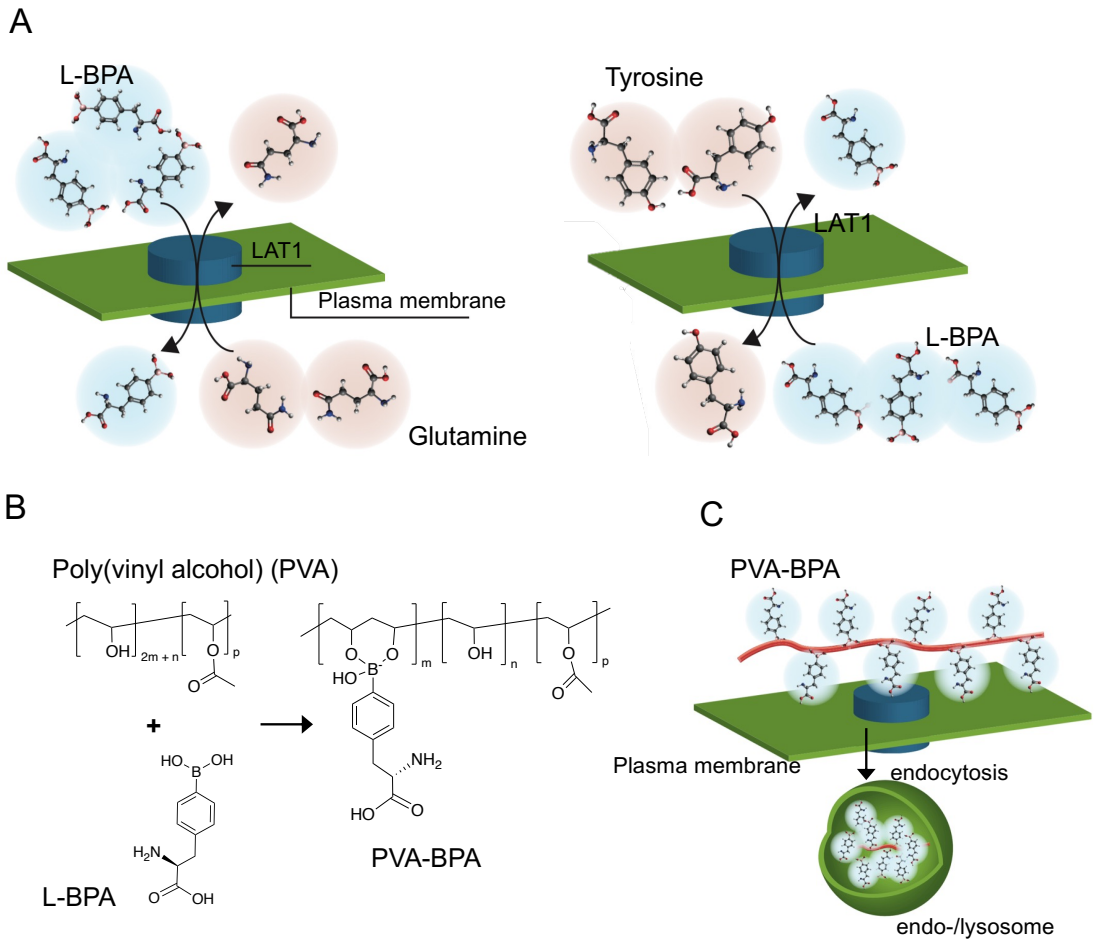


**Figure 1.1.5.3.1 The strategy of PVA-BPA. (A)** Intracellular transport of L-BPA. **(B)** Extracellular transport of L-BPA. **(C)** PVA-BPA is formed by simple mixing in aqueous solution. **(D)** The intracellular distribution of BPA (leftside: fructose-BPA, rightside: PVA-BPA).

## 1.2 Purpose of study

From the previous section, PVA-BPA shows extremely high therapeutic effects, in addition to the very simplicity of manufacturing (PVA) and preparing (just mixing PVA and L-BPA in water). In other words, it can be easily transferred to clinical applications, as a new boron agent for BNCT. Hence, I aim to summarize the systematic knowledge regarding PVA-BPA in doctoral course. Especially, two theme is summarized in this thesis, the basic study of PVA-BPA toward its clinical application, and the functional modification of PVA-BPA by the structural change of BPA.

# CHAPTER 2

# (Optimization of PVA-BPA and evaluation in thoracic tumor model)

# CHAPTER 3

# (The chirality of BPA in PVA-BPA complex)

Relative paper:

Poly(vinyl alcohol) potentiating an inert d-amino acid-based drug for boron neutron capture therapy. *Journal of Controlled Release* (2025) 377: 385-396. DOI: 10.1016/j.jconrel.2024.11.017.

# Preface for chapter 3

Another component of the PVA-BPA complex is the structure of BPA. In this chapter, I have obtained very interesting findings that the pharmacokinetics of PVA-BPA can be significantly changed by replacing the structure of BPA. Hence, here, I summarized the surprising and promising research results, suggesting various insights to drug design.

# 3.1 Introduction

## 3.1.1 BPA and the Chirality

L-4-boronophenylalanine (L-BPA), a boron drug, is an analog of phenylalanine, and therefore exists as an enantiomer called D-4-boronophenylalanine (hereinafter referred to as D-BPA). Coderre JA et al. conducted a distribution study using both enantiomers in a Harding-Passey melanoma cell transplant model and a KHJJ breast cancer cell transplant model in BALB/c mice, then found that L-BPA was more effectively accumulated in tumor tissue than D-BPA [81, 82]. From this background, L-BPA has been used in previous and ongoing clinical studies of BNCT, but D-BPA could not gain attention by researchers in BNCT field.

## 3.1.2 The selectivity of L-BPA against amino acid transporter

L-BPA is recognized by amino acid transporters LAT1, LAT2, and $ATB^{0,+}$ [31], and LAT1 is expressed in many cancer cells [30]. That's why L-BPA has the property of selectively accumulating in tumors. Since a certain level of expression of LAT2 and $ATB^{0,+}$ is observed in normal tissues other than tumor tissues [83, 84], L-BPA shows a certain level of boron accumulation even in normal tissues other than tumor tissues. Hence, depending on the location of the tumor, L-BPA may also accumulate in surrounding normal tissues.

## 3.1.3 Implications of tumor selectivity of boron drugs in BNCT

Even when thermal neutrons are directed at the target tumor, they scatter within the body and cause some nuclear reaction in surrounding normal tissue, causing undesirable

radiation damage. In clinical BNCT, the thermal neutron dose to the target tumor is determined such that the radiation dose generated by the nuclear reaction of boron in the adjacent normal tissue does not exceed its tolerance threshold [85]. That is, the boron concentration in the adjacent normal tissue determines the maximum dose of thermal neutrons, and the higher the boron concentration ratio (T/N ratio) between the tumor and normal tissue, the stronger the BNCT effect on the tumor.

### 3.1.4 Higher LAT1 selectivity of D-enanitomer of BPA

Regarding to transporter selectivity, previously researchers reported studies on amino acid uptake and its selectivity about LAT1 and LAT2 by the use of carbon radioisotope-containing amino acids. And these results have shown that L-phenylalanine is recognized by both LAT1 and LAT2, whereas D-phenylalanine is only by LAT1, but has weaker affinity [86, 87]. Hence, there is possibility that D-BPA, derivative of D-phenylalanine, could interact with LAT1 more selectively than L-BPA. Indeed, Hirai et al. indicated the possibility that $^{18}$F-D-BPA as a PET diagnostic agent showed very low background, indicating negligible interaction of $^{18}$F-D-BPA with normal tissue compared to $^{18}$F-L-BPA [88]. However, the amount of tumor uptake is also very low, confirming D-BPA is not effective and useless for actual BNCT treatment.

### 3.1.5 Purpose of Research

In this chapter, I show that by combination with PVA, this seemingly useless D-BPA can achieve surprisingly high LAT1 selectivity and long-term tumor retention, which is unattainable by the most potent BNCT drug currently available, PVA-L-BPA. I tried to report how this new PVA-BPA complex, PVA-D-BPA, achieved the surprising result as possible as I can. These results reveal that PVA has great potential to induce the latent effects of seemingly inert molecules, and D-amino acid has high potentials as materials for drug carrier, offering the potential for new approaches to drug delivery.

# 3.2 Results

In this chapter, PVA with this chemical properties below were used.
Saponification ratio: 85~89 %, Mn: 10000, Mw: 21100, Mw/Mn: 2.11, (brand name:PE-05JPS)

## 3.2.1 Cellular uptake

First, in order to evaluate the cellular uptake ability in LAT1-positive Human pancreatic cancer-derived BxPC-3 cells [89] or mouse colon cancer-derived CT26 cells [56], sorbitol-L-BPA, PVA-L-BPA, sorbitol-D-BPA, and PVA-D-BPA were incubated with cells for 1, 3, and 6 hours. Then, Intracellular boron uptake in each time point was measured using ICP-MS (**Figure 3.2.1.1**).

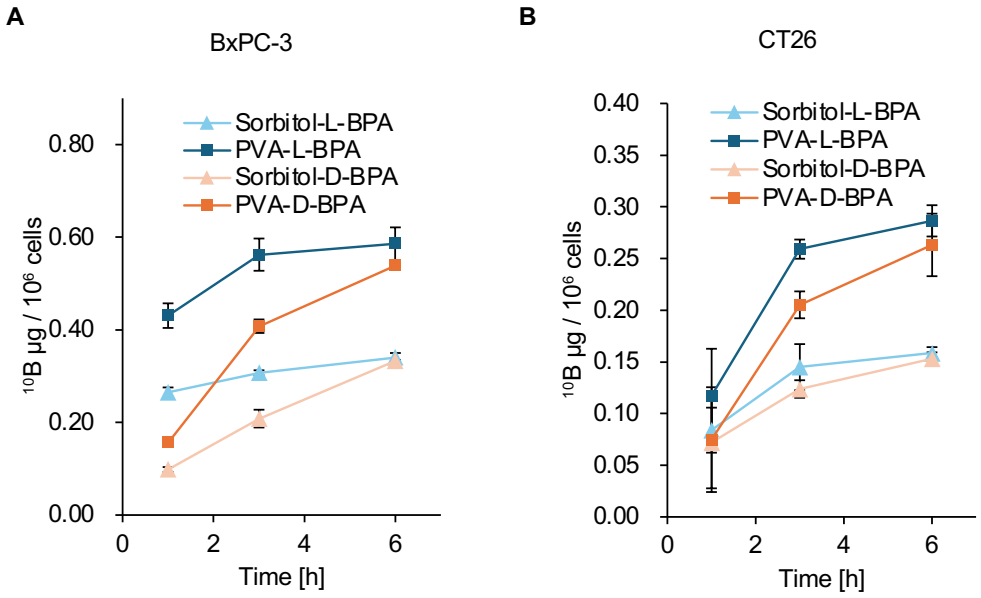


**Figure 3.2.1.1** Cellular uptake in BxPC-3 **(A)** and CT26 cells **(B)**. The results are expressed as means ± SD ($n$ = 3).

Sorbitol-L-BPA showed more efficient cellular uptake than sorbitol-D-BPA, almost reaching a plateau at 3 hours, whereas sorbitol-D-BPA gradually increased its cellular uptake and reached a plateau at 6 hours, showing the same level of cellular uptake as sorbitol-L-BPA. This different kinetics of sorbitol-L/D-BPA can be explained

by the higher affinity of L-phenylalanine for LAT1 than D-phenylalanine [87]. On the other hand, PVA-L-BPA increased uptake compared to sorbitol-L-BPA even after 1 hour incubation and reached a plateau after 3 hours. The amount of uptake increased approximately two-fold, and this is due to the change of uptake behavior from antiport mechanism through LAT1 to LAT1-mediated endocytosis. Furthermore, previous studies have demonstrated that polymers with multiple substrates of amino acid transporters in their side chains can interact multivalently with the corresponding transporters and enhance their uptake into cells [90-92]. Hence, PVA-L-BPA may also induce such multivalent effects like this. Importantly, in line with such a mechanism, PVA also increased D-BPA uptake approximately 2-fold.

Although PVA-D-BPA was taken up into cells more slowly than PVA-L-BPA, it showed similar uptake after 6 hours. Similar results were also obtained with LAT1-positive mouse colon cancer (CT26) cells (**Figure 3.2.1.1 B**), suggesting that the enantiomers have different affinities for cancer cells.

## 3.2.2 Specificity

Next, in order to evaluate the LAT1 dependence of cellular uptake of each sample, the cellular uptake amount of boron after 3 hours incubaiton with the presence of a LAT1 inhibitor was evaluated. The LAT1 inhibitors used in this experiment were 2-aminobicyclo(2,2,1)heptane-2-carboxylic acid (BCH) and JPH203. BCH is a system L inhibitor, and upon uptake, competitively inhibits LAT1 and LAT2 [40]. On the other hand, JPH203 is a LAT1-specific inhibitor [93] (**Figure 3.2.2.1**).

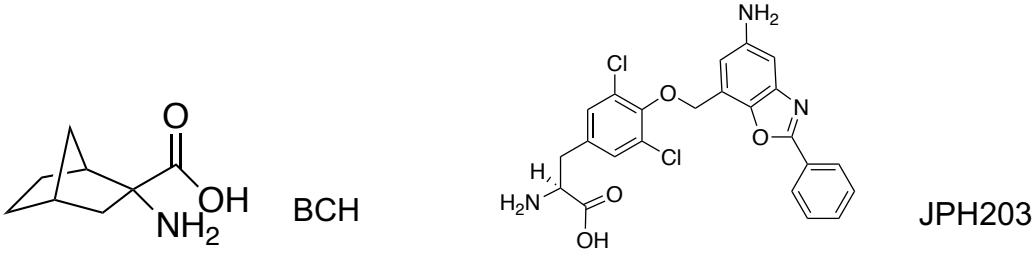


**Figure.3.2.2.1 The Chemical structures of BCH and JPH203.**

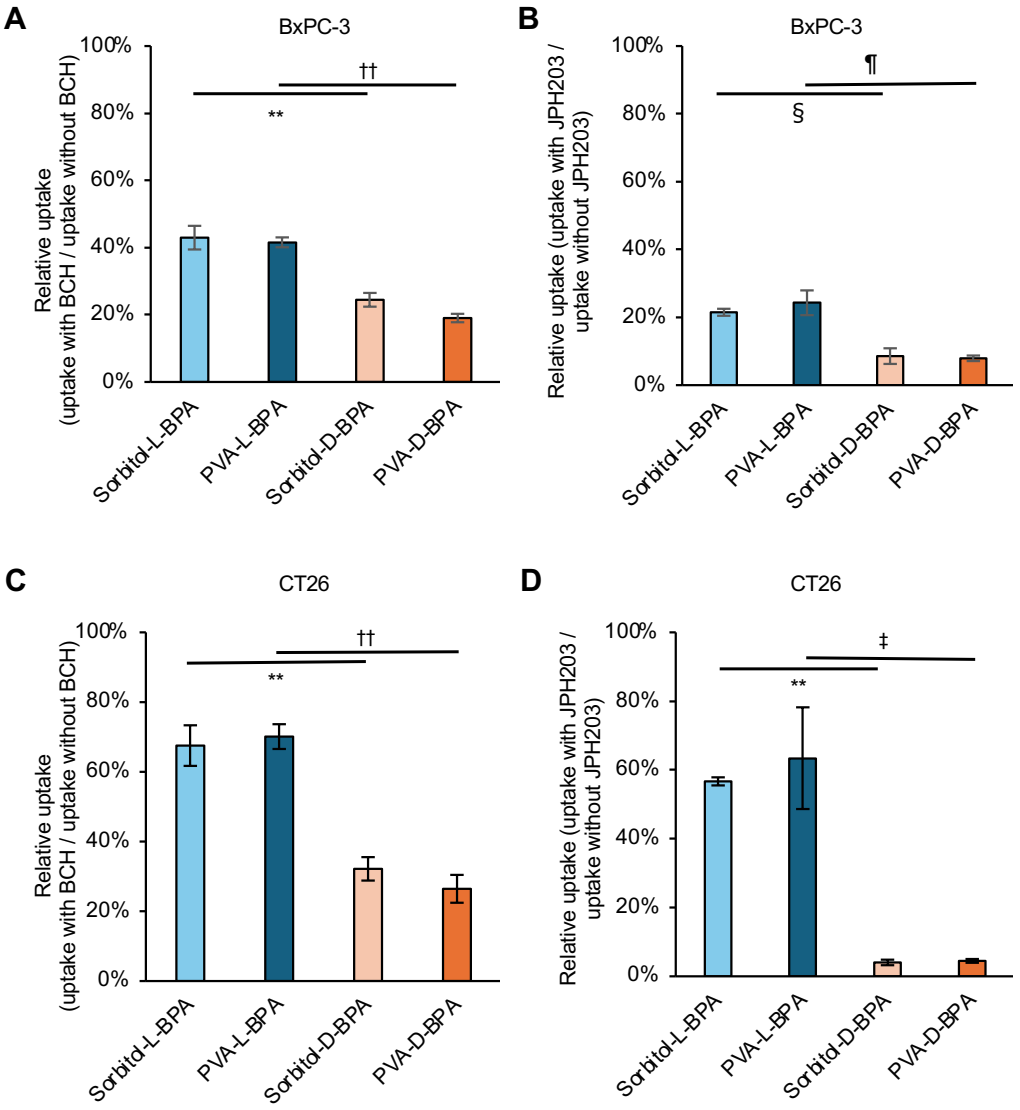


**Figure.3.2.2.2 Inhibition assay.** (**A** and **B**) Inhibition study with BCH and JPH203 in BxPC-3. (**C** and **D**) Inhibition study with BCH and JPH 203 in CT26 cells. The cells were incubated with each sample for 3 h with/without the inhibitor. The relative uptake was calculated as the ratio of uptake with to without the inhibitor. The results are expressed as means ± SD ($n = 3$). *$p < 0.05$, †$p < 0.01$, ‡$p < 0.005$, §$p < 0.001$, ¶$p < 0.0001$, **$p < 0.00005$, ††$p < 0.00001$ (one-way ANOVA with Tukey's multiple comparison test).

As demonstrated in **Figure 3.2.2.2 A** and **C**, BCH significantly reduced the cellular uptake rate of all samples in both BxPC-3 and CT26 cells, indicating

involvement of system L transporters. Notably, BCH had a more pronounced inhibitory effect on D-BPA compared to L-BPA, as L-BPA can utilize $ATB^{0,+}$ for internalization, whereas D-BPA may not. To explore this further, JPH203, was employed next. In BxPC-3 cells (**Figure 3.2.2.2B**), JPH203 reduced the uptake of sorbitol-L-BPA and PVA-L-BPA by ~78%, whereas sorbitol-D-BPA and PVA-D-BPA exhibited a more substantial reduction (~92%). The limited inhibition of L-BPA is attributed to LAT2 and $ATB^{0,+}$ transport. This suggests that PVA-L-BPA may enter cells through LAT2/$ATB^{0,+}$ in addition to LAT1-mediated endocytosis. The dramatic inhibition of D-BPA uptake highlights the high specificity of sorbitol-D-BPA and PVA-D-BPA to LAT1. A similar pattern was observed in CT26 cells (**Figure 3.2.2.2D**), with ~40% inhibition for L-BPA and ~95% for D-BPA, further supporting specificity of D-BPA to LAT1.

## 3.2.3 Internalization process and subcellular distribution

Subcellular localization was investigated in BxPC-3 cells using confocal laser scanning microscopy (CLSM). After a 0.5-hour incubation, lysosomes and L-/D-BPA were visualized with Lysotracker Red DND-99 and 5-(diethylamino)-2-((methylimino)methyl)phenol (DAHMI) [94], respectively (**Figure 3.2.3.1**). Sorbitol-L-/D-BPA localized to the cytosol, whereas Cy5-PVA-L-/D-BPA accumulated in lysosomes. These results indicate that sorbitol-L-/D-BPA likely entered via amino acid transporters, while PVA-L-/D-BPA may have utilized transporter-mediated endocytosis.

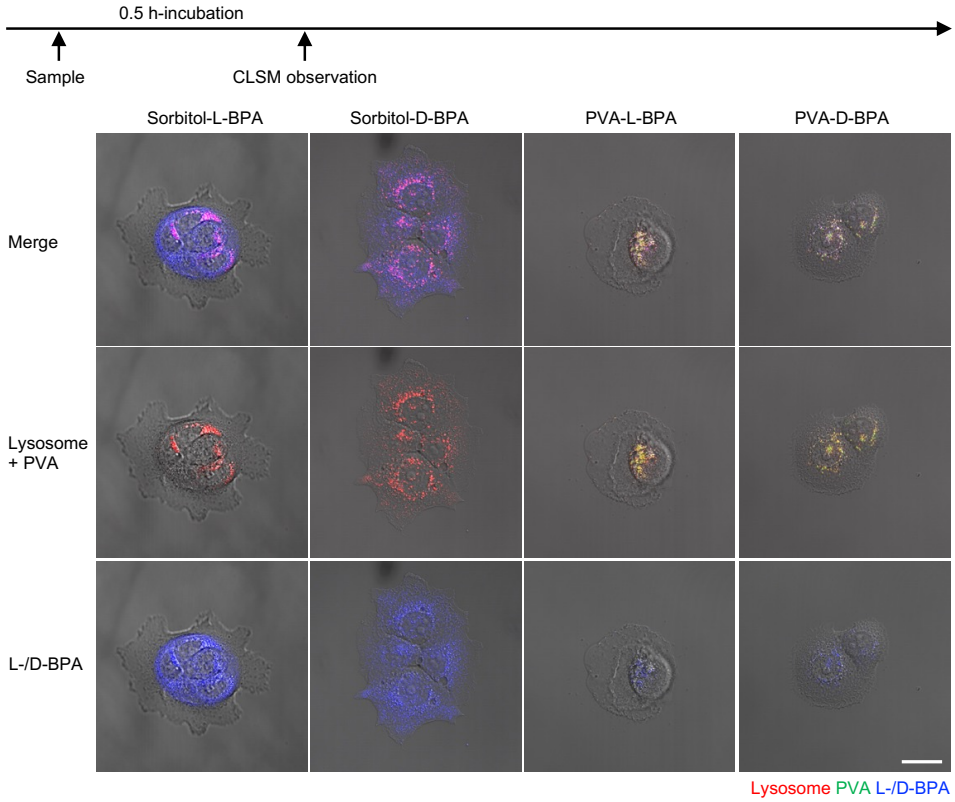


**Figure 3.2.3.1 Fluorescence microscopy images of BxPC-3 cells.** BxPC-3 cells were incubated with samples for 0.5 h. Endo-/lysosomes and L-/D-BPA were labeled using LysoTracker Red DND-99 and DAHMI, respectively. Scale bar, 20 µm.

## 3.2.4 Subcellular transition

Next, to evaluate the transition of subcellular distribution, cells were incubated with the samples for 3 h, followed by 0.5 h in fresh cell culture medium (**Figure 3.2.4.1**). It was assumed that this additional 0.5 hour incubation would eliminate intracellular L-/D-BPA.

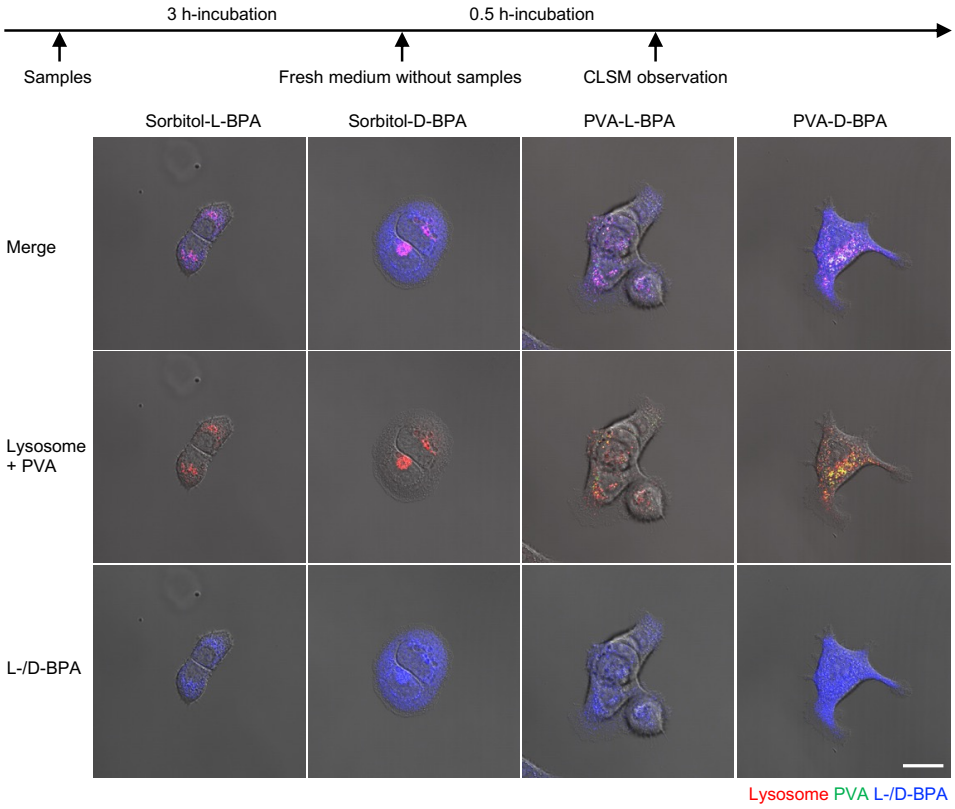


**Figure 3.2.4.1 Confocal laser scanning microscopic images of BxPC-3 cells.** Subcellular transition. The cells were incubated with each sample for 3 h, and additionally incubated in fresh medium for 0.5 h. Endo-/lysosomes and L-/D-BPA were labeled using LysoTracker Red DND-99 and DAHMI, respectively. Scale bar, 20 μm.

After 3 hours of incubation and following incubation by 0.5 hours in fresh medium, sorbitol-L-BPA fluorescence decreased (**Figure 3.2.4.1**), likely due to LAT1 antiport-mediated efflux. For Cy5-PVA-L-/D-BPA, Cy5-PVA remained in lysosomes, while L-/D-BPA diffused into the cytosol, potentially due to pH-sensitive cleavage of the boronate ester bond in lysosomes [95]. The fluorescence of PVA-D-BPA exceeded that of PVA-L-BPA, and sorbitol-D-BPA showed higher fluorescence compared to sorbitol-/PVA-L-BPA. These findings suggest prolonged intracellular retention of D-BPA.

## 3.2.5 Intracellular retention

To quantitatively examine intracellular retention, BxPC-3 cells were incubated with the sample for 3 hours and further incubated in fresh cell culture medium without sample for 0.5 hour (**Figure 3.2.5.1**).

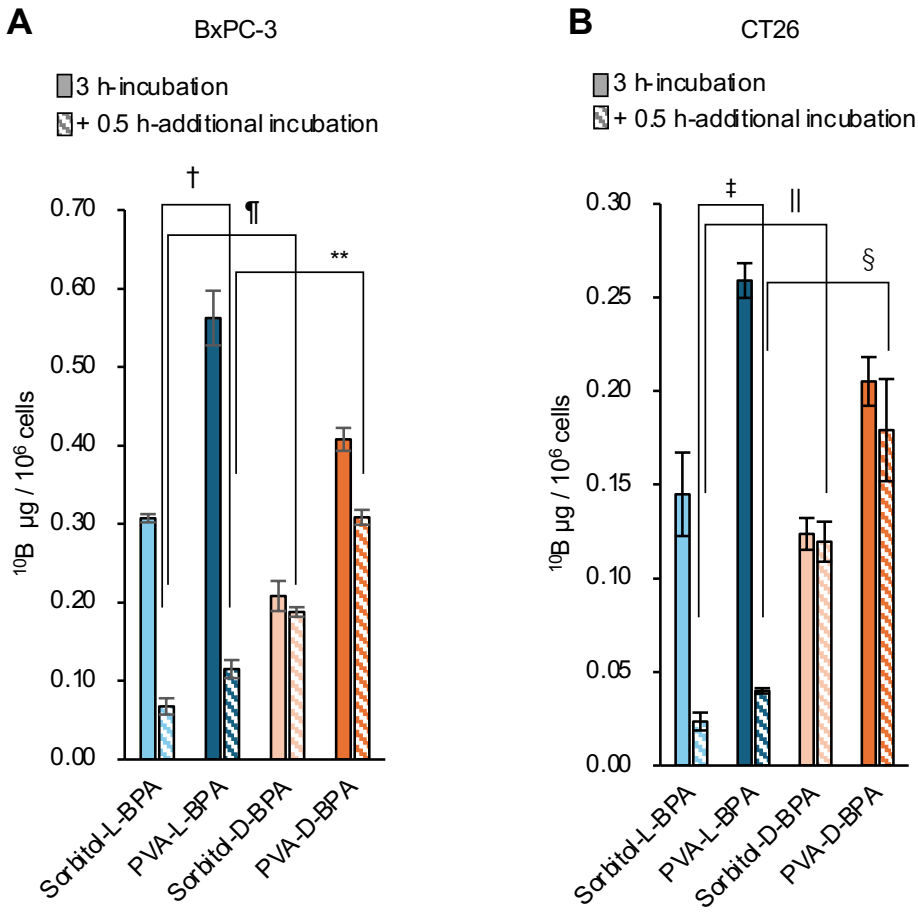


**Figure 3.2.5.1 Intracellular retention in (A) BxPC-3 and (B) CT-26 cells.** The cells were incubated with each sample for 3 h, and additionally incubated in fresh medium for 0.5 h. The results are expressed as means ± SD ($n$ = 3). *$p < 0.05$, †$p < 0.01$, ‡$p < 0.005$, §$p < 0.001$, ||$p < 0.0005$, ¶$p < 0.0001$, **$p < 0.00005$ (Student's $t$-test).

Additional incubation significantly reduced the intracellular boron concentration of sorbitol-L-BPA and PVA-L-BPA, but PVA-L-BPA showed higher intracellular boron content, which is consistent with previous studies [42]. Surprisingly, sorbitol-D-BPA and

PVA-D-BPA showed significantly higher intracellular retention than sorbitol-/PVA-L-BPA, which was consistent with CLSM observations (**Figure 3.2.3.1**).

Here, in order to investigate what causes high intracellular retention ability of D-BPA, we observed its retention behavior over a longer period of time and also observed its retention behavior by inhibiting LAT1. Specifically, after incubating with the sample for 3 hours, the cells were incubated with fresh cell culture medium for 2 hours (with or without LAT1 inhibitor, JPH203), and then the amount of boron remaining in the cells was quantified (**Figure 3.2.5.2**).

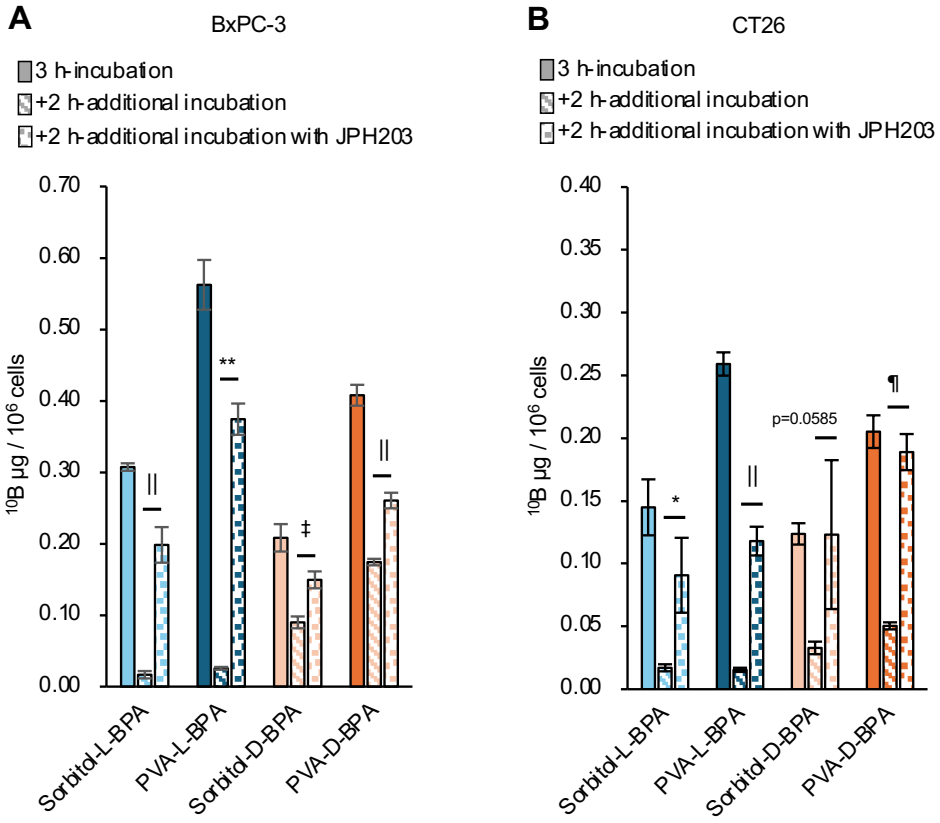


**Figure 3.2.5.2 Intracellular retention with JPH203 in (A) BxPC-3 and (B) CT-26 cells.** The cells were incubated with each sample for 3 h, and 2 h-additional incubation in fresh medium with/without JPH203 followed. The results are expressed as means ± SD ($n$ = 3). *$p$ < 0.05, †$p$ < 0.01, ‡$p$ < 0.005, §$p$ < 0.001, ‖$p$ < 0.0005, ¶$p$ < 0.0001, **$p$ < 0.00005 (Student's $t$-test).

Most boron atoms were excreted from cells treated with sorbitol-/PVA-L-BPA (~0.020

$^{10}$B μg/$10^6$ cells), whereas 43% of boron atoms were retained in cells treated with sorbitol-/PVA-D-BPA after 2 hours of additional incubation. These results strongly indicate that sorbitol-/PVA-D-BPA excretion is significantly slower. This is probably because D-BPA is released from PVA-D-BPA and translocated to the cytoplasm similarly to sorbitol-D-BPA, reverting the lower transport efficiency through LAT1 than L-BPA. Then, to confirm whether LAT1 relates to the high intracellular retention and efflux pathway, LAT1 was inhibited using JPH203 during the 2 h-additional incubation in fresh cell culture medium not containing boron samples (**Figure 3.2.4.1**). As a result, all samples showed significant improvement in the retention. This indicates that LAT1 is significantly involved in the excretion of L-/D-BPA and that transport efficiency is important for intracellular retention. Furthermore, the inhibitory effect of JPH203 was somewhat limited in the PVA group compared to the sorbitol group, regardless of the enantiomer, probably because PVA-L/D-BPA may also be excreted outside the cells by transcytosis. A similar trend to the aforementioned results was also obtained in CT26 cells (**Figure 3.2.5.2 B**).

## 3.2.6 Biodistribution study

The biodistribution was assessed in BALB/c mice with subcutaneous CT26 tumors. Samples were administered intravenously via the tail vein at a dose of 10 mg L-/D-BPA per mouse, and boron concentrations in tumors and organs were quantified using ICP-MS (**Figure 3.2.6.1**).

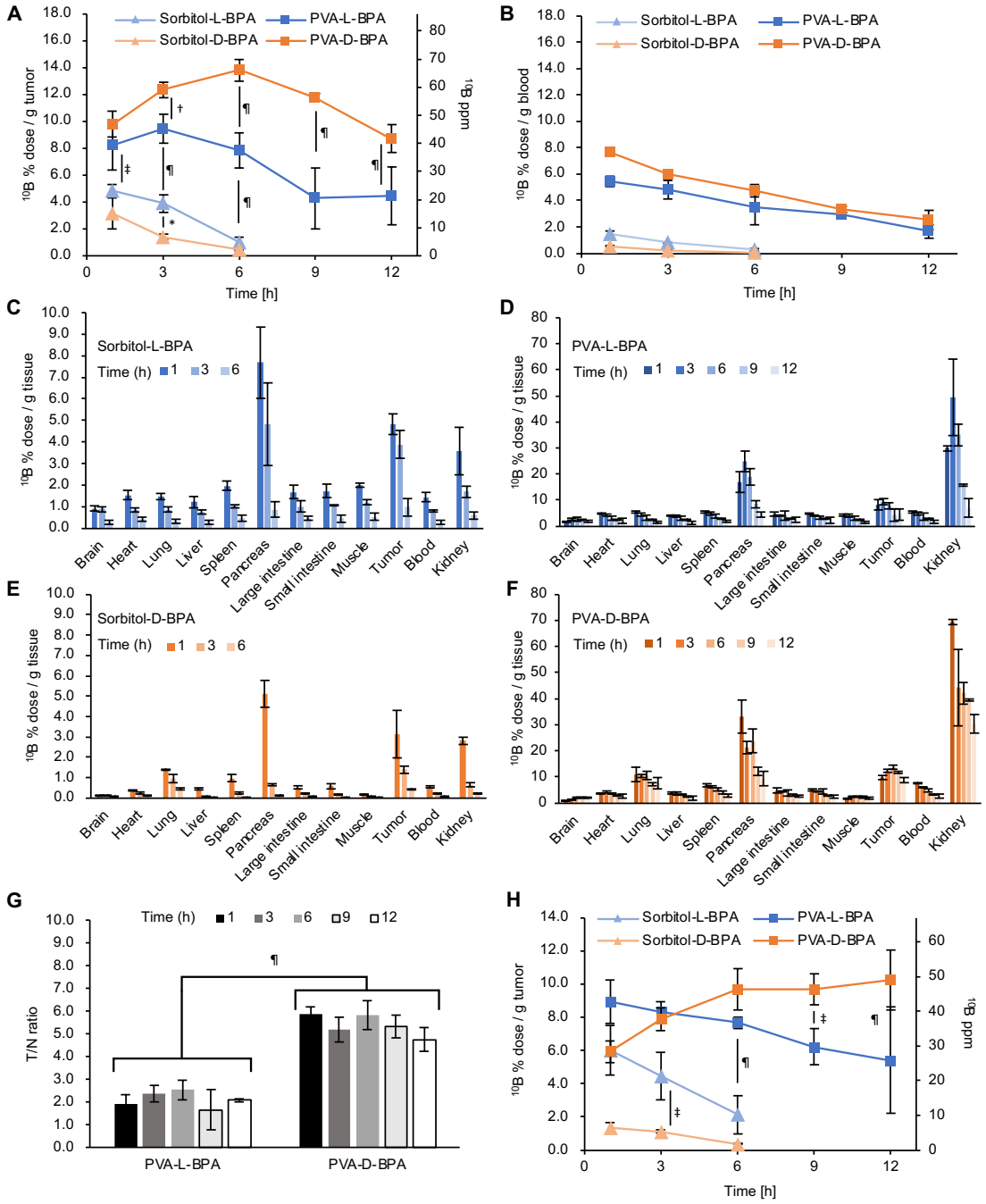


**Figure 3.2.6.1 Biodistribution. (A, B)** Boron concentration within **(A)** tumor and **(B)** blood in subcutaneous CT26 tumor models. **(C-F)** Distribution of boron in case of sorbitol-L-BPA **(C)**, PVA-L-BPA **(D)**, sorbitol-D-BPA **(E)** and PVA-D-BPA **(F)**. **(G)** The ratio of boron concentration between tumor and muscle (T/N ratio). **(H)** Boron concentration within tumor in subcutaneous BxPC-3 tumor models. The results are

expressed as means ± SD ($n$ = 3). *$p$ < 0.05, †$p$ < 0.01, ‡$p$ < 0.005, ¶$p$ < 0.0001 (two-way ANOVA with Tukey's multiple comparison test).

In tumors (**Figure 3.2.6.1 A**), sorbitol-L-BPA showed immediate accumulation after administration, followed by a gradual decline due to efflux, reaching ~1% dose/g tumor at 6 hours post-injection. PVA-L-BPA exhibited rapid accumulation and sustained retention, maintaining ≥ ~7.8% dose/g tumor within 6 hours, consistent with previous findings [42]. Sorbitol-D-BPA reached ≤ ~3.1% dose/g tumor, below the clinical threshold (≥ 5.3% dose/g tumor, or ≥ 25 ppm boron) [65]. Remarkably, PVA enhanced the tumor accumulation of D-BPA. PVA-D-BPA showed higher accumulation (~14% dose/g tumor) and longer retention than PVA-L-BPA at 6 hours post-injection. This can be attributed to improved cellular uptake and retention in tumor cells, as observed in *in vitro* studies (**Figure 3.2.1.1** and **Figure 3.2.5.1**).

Regarding blood circulation (**Figure 3.2.6.1 B**), sorbitol-L/D-BPA were rapidly cleared by renal excretion due to their low molecular weight. However, PVA complexes increased molecular weight, reducing renal clearance and prolonging circulation [55]. These circulation profiles likely influenced tumor accumulation. For sorbitol-L/D-BPA, rapid clearance within 1 hour limited tumor exposure to high concentrations during that time, with transport efficiency being a key factor. Hence, sorbitol-L-BPA, being more efficiently taken up by cancer cells than sorbitol-D-BPA (**Figure 3.2.1.1**), showed higher tumor accumulation. On the other hand, for PVA-L/D-BPA, gradual blood concentration decreases over 12 hours resulted in intracellular retention playing a critical role in tumor accumulation levels. The superior retention of PVA-D-BPA (**Figure 3.2.5.1**) likely explains its higher tumor accumulation at 6 hours post-injection.

In normal organs (**Figure 3.2.6.1 C–F**), all samples accumulated significantly in the kidney and pancreas, consistent with renal excretion pathways and LAT1 expression in the basolateral membrane of the pancreas [57]. Sorbitol-D-BPA showed negligible accumulation in LAT1-negative organs, indicating high LAT1 specificity. PVA moderately increased D-BPA accumulation in all organs due to prolonged circulation. Notably, PVA-D-BPA exhibited significantly higher Tumor / Normal tissue (T/N) ratios than PVA-L-BPA (**Figure 3.2.6.1 G**), reflecting LAT1 specificity of D-BPA. Unexpectedly, sorbitol-/PVA-D-BPA accumulated in the lungs to some extent

(**Figure 3.2.6.1 E, F**). While the mechanism remains unclear, a lung protein other than LAT1 might recognize D-BPA, warranting further investigation.

Subcutaneous BxPC-3 tumors in BALB/c nude mice were also evaluated (**Figure 3.2.6.1 H**). This tumor model, characterized by hypovascular and stroma-rich tissue, hinders nanoparticle extravasation and penetration [54, 96]. Consistent with our previous findings [42], PVA-L-BPA achieved efficient tumor accumulation despite these barriers, due to its smaller size compared to typical nanoparticles. Interestingly, PVA-D-BPA showed slower accumulation and longer retention in these tumors, consistent with BxPC-3 cellular uptake experiments, where PVA-D-BPA demonstrated gradual cellular uptake (**Figure 3.2.1.1**) and higher retention in BxPC-3 cells (**Figure 3.2.6.2**). These results suggest that PVA-D-BPA retains its extravasation and penetration ability, and the differences in accumulation and retention should be tumor-cell-specific, likely influenced by transporter expression and endocytosis kinetics.

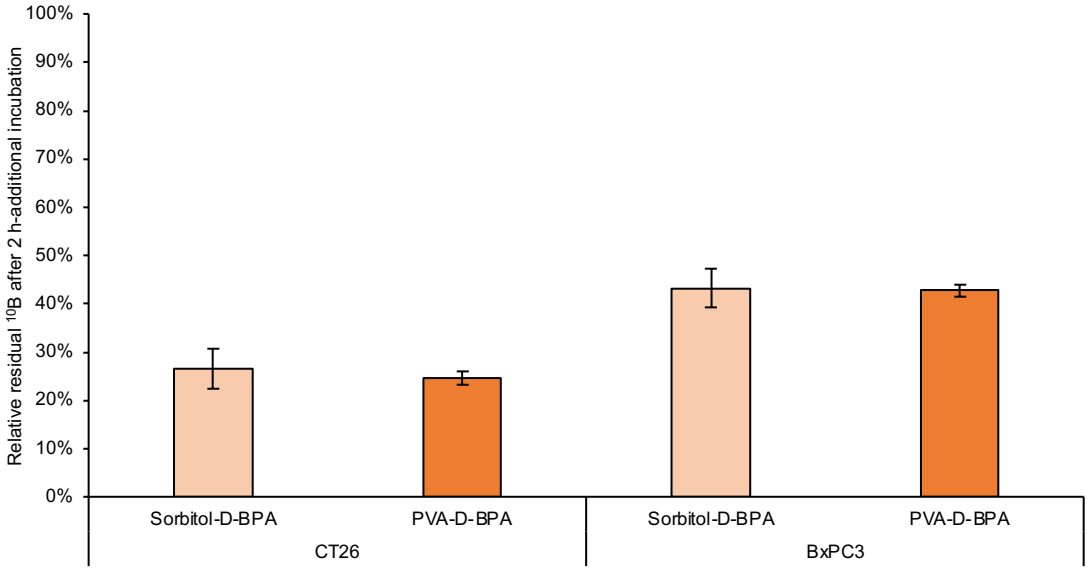


**Figure 3.2.6.2 Comparing intracellular retention of sorbitol-/PVA-D-BPA for 2 hours in CT26 and BxPC-3 cell line.** Cells were incubated with each sample for 3 h, and additionally incubated in fresh medium for 2 h. The results were expressed as percentages of residual $^{10}$B to original amount at 3 h incubation. The results are expressed as means ± SD ($n$ = 3).

## 3.2.7 Neutron capture therapy

Antitumor effects were tested in CT26 tumor-bearing BALB/c mice. Samples were administered via tail vein injection (10 mg BPA / mouse, here the body weight of mouse was assumed as 20g and equivalent to 500 mg/kg), followed by thermal neutron irradiation 3 hours later (**Figure 3.2.7.1 A, B**). Sorbitol-L-BPA suppressed tumor growth until day 15, completely curing 3 of 6 tumors, though the remaining tumors regrew. PVA-L-BPA also cured 3 tumors, with regrowth significantly suppressed in the others. Sorbitol-D-BPA showed weaker antitumor effects due to insufficient tumor accumulation. In contrast, PVA-D-BPA cured 5 of 6 tumors completely, with the remaining tumor being significantly smaller 33 days post-irradiation. These outcomes align with intratumoral boron concentrations (**Figure 3.2.6.1 A**).

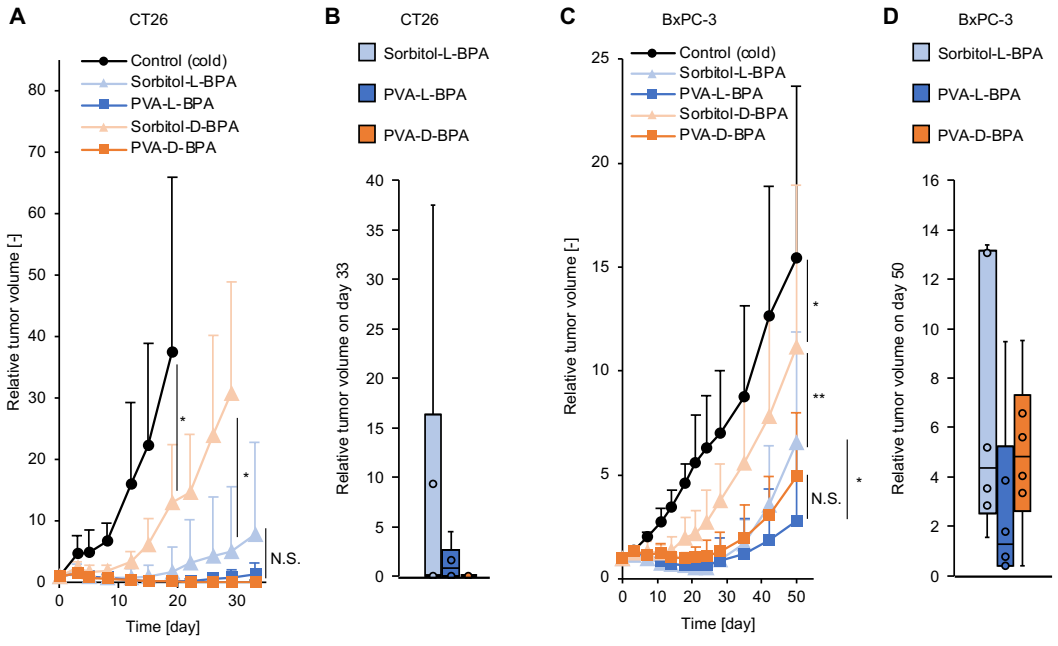


**E**

| Sample | Injected dose (BPA mg/kg) | Interval between injection and irradiation | T/N ratio (tumor/ muscle) | Estimated $^{10}$B concentration in the muscle | Estimated $^{10}$B concentration in the tumor |
|---|---|---|---|---|---|
| PVA-L-BPA | 340 | 3 h | 1.87 | 14.4 ppm | 26.9 ppm |
| PVA-D-BPA | 500 | 6 h | 3.21 | 14.4 ppm | 46.3 ppm |

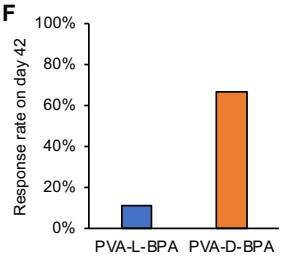


**Figure 3.2.7.1 Antitumor effects. (A, B)** Tumor growth curves untill day 33 **(A)** and box-and-whisker plots on day 33 after the irradiation **(B)** in subcutaneous CT26 tumor mouse models. The samples were intravenously injected, then the tumors were

irradiated with thermal neutrons 3 h after the injection, and the day is annotated as day 0. The sorbitol-D-BPA and groups of control (cold) were euthanized on day 29 and 19 for the endpoint, respectively. **(C, D)** Tumor growth curves by day 50 and **(C)** box-and-whisker plots on day 50 **(D)** in subcutaneous BxPC-3 tumor mouse models. 3h after the intravenously injection of samples, tumors were irradiated with thermal neutrons to sorbitol-L-BPA, PVA-L-BPA and sorbitol-D-BPA on day 0. PVA-D-BPA group were irradiated with thermal neutrons 6 h after injection. The results are expressed as means ± SD ($n = 6$). *$p < 0.05$, **$p < 0.01$ (two-way ANOVA with Tukey's multiple comparisons test). **(E)** A scheme table showing an experimental condition that mimicked the clinical situation. **(F)** Response rate on PVA-L-BPA and PVA-D-BPA 42 days after treatment in the BxPC-3 mouse model. This experiment condition mimicked a clinical situation. The response rate was defined as the percentage of mice whose tumors shrank from their original size ($n = 9$).

Body weights across irradiated groups dropped slightly 3–5 days post-irradiation but returned to baseline levels (**Figure 3.2.7.2**). This temporary weight loss was likely due to anorexia, a common radiotherapy side effect.

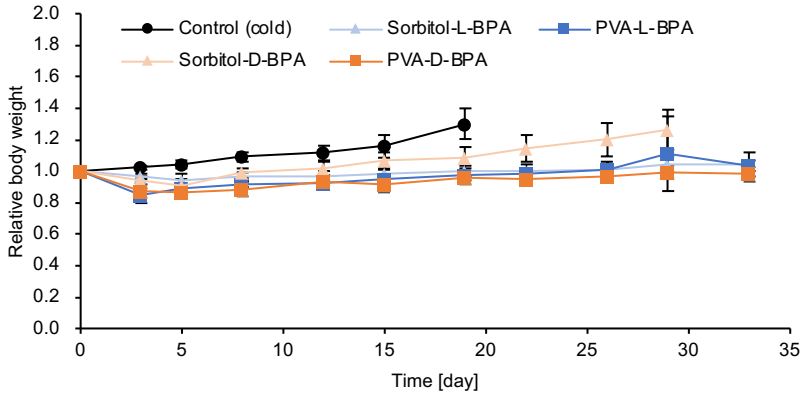


**Figure 3.2.7.2 Relative weight of CT26 model mice.** The groups of sorbitol-D-BPA and control (cold) were euthanized on day 29 and 19 for the endpoint respectively. The results are expressed as means ± SD ($n = 6$).

BNCT effects were also evaluated in subcutaneous BxPC-3 tumor-bearing BALB/c nude mice (**Figure 3.2.7.1 C, D**). Here, 3 hours after the injection of sorbitol-L-BPA, PVA-L-BPA, and sorbitol-D-BPA, or 6 hours after the injection of PVA-D-BPA, neutron irradiation was performed. As a result, sorbitol-L-BPA inhibited tumor growth but showed moderate regrowth from day 28. PVA-L-BPA improved therapeutic efficacy, significantly suppressing regrowth, consistent with biodistribution data (**Figure 3.2.6.1 H**). For D-BPA, sorbitol-D-BPA exhibited moderate effects, while PVA-D-BPA demonstrated significantly enhanced antitumor activity comparable to PVA-L-BPA.

Although PVA-D-BPA's effects did not surpass PVA-L-BPA under these conditions, its higher T/N ratios (**Figure 3.2.6.1 G**) suggest potential advantages in practical applications. To test this, injections were adjusted to equalize boron concentrations in muscle tissue, representative normal tissue, at the time of neutron irradiation, mimicking clinical conditions (**Figure 3.2.7.1 E**). As higher T/N ratios correlate with greater intratumoral boron concentrations. As a results, PVA-D-BPA achieved a higher response rate (67%) than PVA-L-BPA (11%) at 42 days post-BNCT (**Figure 3.2.7.1F**).

## 3.3Discussion

Research on D-amino acids in mammals is relatively recent, with earlier studies predominantly focusing on their use as inert materials. It has been frequently reported that D-amino acids interact less with biological components and cells compared to their L-isomer [97-102]. Additionally, D-amino acids are widely utilized to enhance the stability of peptides by protecting them from enzymatic degradation. On the other hand, some studies highlight the unique biological roles of D-amino acids. For instance, D-serine functions as a co-agonist for receptors involved in learning, memory, and behavior, while D-aspartate serves as a neurotransmitter or neuromodulator in the nervous system [103]. In cancer research, D-amino acids have shown potential as biomarkers for early diagnosis and therapeutic agents by inhibiting protein synthesis or generating reactive oxygen species via D-amino acid oxidase [104]. However, none of these studies have demonstrated strong antitumor effects capable of completely curing tumors, nor utilizing the high intracellular retention due to the affinity against amino acid transporter.

In this study, we leveraged the distinct properties of D-BPA in combination with PVA, showcasing unprecedented tumor-selective delivery, prolonged intratumoral retention, and complete tumor eradication. PVA played a crucial role in this approach. By forming a complex with D-BPA, PVA moderately extended the drug's circulation time, facilitating prolonged interaction time with tumors. Additionally, PVA altered the uptake mechanism to LAT1-mediated endocytosis, significantly enhancing tumor accumulation. The acidic microenvironment in endo-/lysosome triggered the cleavage of the boronate ester bond and release free D-BPA, thereby reverting its low affinity and critically preventing the efflux (**Figure 3.3.1**). Remarkably, these outcomes were achieved simply by mixing PVA and D-BPA in an aqueous solution.

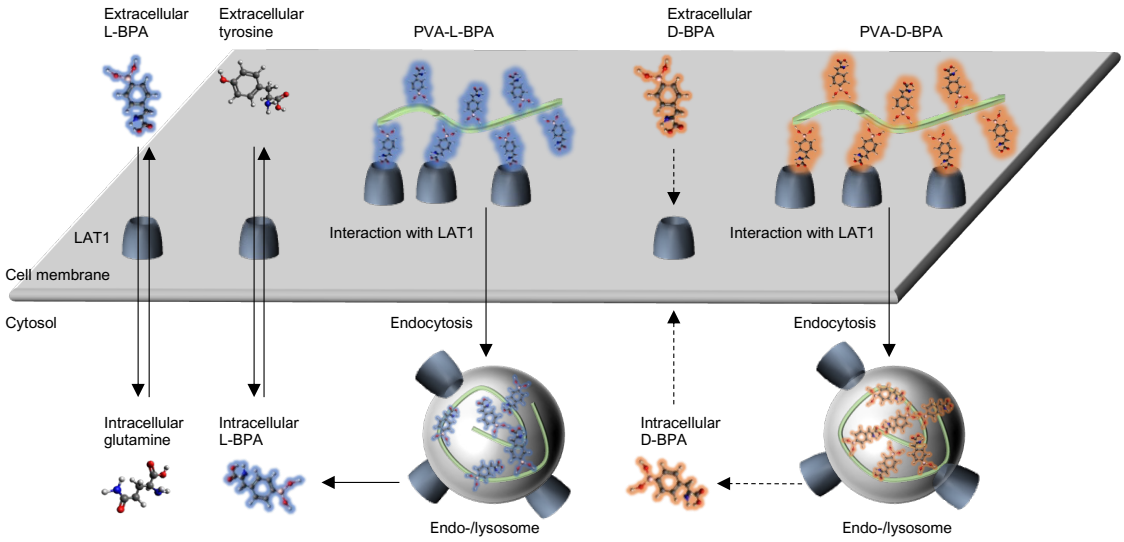


**Figure 3.3.1 Schematic illustration of cell internalization and efflux of PVA-L-/D-BPA.** LAT1 operates via an antiport mechanism. L-BPA, when present at a high extracellular concentration, is efficiently taken up by exchanging with intracellular substrates like glutamine. In contrast, at low extracellular concentrations, intracellular L-BPA is quickly exported in exchange for extracellular substrates such as tyrosine. PVA-L-BPA, however, interacts with LAT1 and is internalized through LAT1-mediated endocytosis. Within the acidic environment of endosomes or lysosomes, PVA-L-BPA dissociates into PVA and L-BPA. The released L-BPA gradually diffuses into the cytosol, where it is subject to LAT1-mediated antiport, delaying its efflux to some extent. On the other hand, D-BPA shows high specificity for LAT1 but has lower transport efficiency compared to the L-enantiomer. PVA enhances the cellular uptake of D-BPA through multivalent interactions. PVA-D-BPA undergoes LAT1-mediated endocytosis and dissociates into PVA and D-BPA in response to acidic conditions. However, unlike L-BPA, the lower transport efficiency of D-BPA significantly slows unfavorable LAT1-mediated transport, resulting in prolonged intracellular retention.

PVA was traditionally used as a biocompatible material to minimize undesired interactions in drug delivery, Indeed, it prevent the cellular uptake of nanoparticle and not taken up by cell itself [105]. However, we found that PVA enhances the efficacy of seemingly ineffective drugs, presenting a novel approach for drug delivery system design. Such unconventional use of PVA sometimes brings innovative serendipity even

in the other research field. For example, PVA has been shown to act as an efficient substitute for serum albumin in the ex vivo expansion of hematopoietic stem cells [106]. This suggests that PVA may have additional unexplored applications.

By utilizing LAT1-specific targeting, PVA-D-BPA achieved a high tumor-to-normal tissue (T/N) ratio, a critical parameter for clinical BNCT to minimize radiation exposure to surrounding normal tissues. Increasing tumor drug concentration without improving the T/N ratio may result in higher radiation doses to normal tissues, limiting therapeutic efficacy. Nanoparticles relying on prolonged circulation and enhanced permeability and retention (EPR) effects have shown limited improvement in clinical settings due to unchanged T/N ratios and concerns about formulation safety [107].

Our experiments demonstrated the superior intratumoral retention of PVA-D-BPA without requiring infusion, as with sorbitol-L-BPA, and its higher T/N ratio compared to PVA-L-BPA. However, L-BPA may be advantageous in targeting heterogeneous tumors with LAT1-negative cells, as it can also interact with LAT2 and $ATB^{0,+}$. For clinical application, assessing LAT1 expression heterogeneity through tissue analysis or imaging techniques like PET with $^{18}F$-labeled BPA could provide critical information for optimizing BNCT. Also, combination of multiple kind of boron drug should be more effective, because it has been shown that co-administration of boron compound called BSH, which does not target LAT1, and L-BPA, achieved a more uniform distribution of boron within the tumor and improve therapeutic efficacy compared to L-BPA alone [108].

By combining different formulations of PVA/sorbitol-L-/D-BPA, tailored strategies can be developed for specific tumor types and locations. Although $^{18}F$'s short half-life poses challenges, the simplicity of PVA-based systems offers a feasible solution for individualized BNCT.

# CHAPTER 4

# (Summary and future perspective)

# CHAPTER 5

# (Materials and Methods, and Appendix)

## Preface for chapter 5

Here, we will provide detailed experimental methods for the experimental results described in this thesis, as well as experimental results that serve as an addendum to this thesis.

# REFERENCES


1. Bray, F. et al. Global cancer statistics 2022: GLOBOCAN estimates of incidence and mortality worldwide for 36 cancers in 185 countries. *CA Cancer J Clin* **74**, 229-263 (2024).
2. Bray, F., Laversanne, M., Weiderpass, E. & Soerjomataram, I. The ever-increasing importance of cancer as a leading cause of premature death worldwide. *Cancer* **127**, 3029-3030 (2021).
3. Chen, S. et al. Estimates and Projections of the Global Economic Cost of 29 Cancers in 204 Countries and Territories From 2020 to 2050. *JAMA Oncol* **9**, 465-472 (2023).
4. Guida, F. et al. Global and regional estimates of orphans attributed to maternal cancer mortality in 2020. *Nat Med* **28**, 2563-2572 (2022).
5. Abbas, Z. & Rehman, S. An Overview of Cancer Treatment Modalities. *Neoplasm* **1**, 138-157 (2018).
6. Wagner, A., Ploder, O., Enislidis, G., Truppe, M. & Ewers, R. Virtual image guided navigation in tumor surgery- technical innovation. *J Craniomaxillofac Surg* **23**, 271-273 (1995).
7. Debela, D.T. et al. New approaches and procedures for cancer treatment: Current perspectives. *SAGE Open Med* **9**, 20503121211034366 (2021).
8. Xia, Y., Sun, M., Huang, H. & Jin, W.L. Drug repurposing for cancer therapy. *Signal Transduct Target Ther* **9**, 92 (2024).
9. Mitchell, M.J. et al. Engineering precision nanoparticles for drug delivery. *Nat Rev Drug Discov* **20**, 101-124 (2021).
10. Jain, R.K. TRANSPORT OF MOLECULES IN THE TUMOR INTERSTITIUM - A REVIEW. *Cancer Research* **47**, 3039-3051 (1987).
11. Choi, H.S. et al. Renal clearance of quantum dots. *Nat Biotechnol* **25**, 1165-1170 (2007).
12. Maeda, H., Wu, J., Sawa, T., Matsumura, Y. & Hori, K. Tumor vascular permeability and the EPR effect in macromolecular therapeutics: a review. *J Control Release* **65**, 271-284 (2000).
13. Anselmo, A.C. & Mitragotri, S. Nanoparticles in the clinic: An update. *Bioeng*

*Transl Med* **4**, e10143 (2019).

14. Pawlik, T.M. & Keyomarsi, K. Role of cell cycle in mediating sensitivity to radiotherapy. *International Journal of Radiation Oncology Biology Physics* **59**, 928-942 (2004).
15. Thomlinson, R.H. & Gray, L.H. THE HISTOLOGICAL STRUCTURE OF SOME HUMAN LUNG CANCERS AND THE POSSIBLE IMPLICATIONS FOR RADIOTHERAPY. *British Journal of Cancer* **9**, 539-& (1955).
16. Gray, L.H., Conger, A.D., Ebert, M., Hornsey, S. & Scott, O.C.A. THE CONCENTRATION OF OXYGEN DISSOLVED IN TISSUES AT THE TIME OF IRRADIATION AS A FACTOR IN RADIOTHERAPY. *British Journal of Radiology* **26**, 638-648 (1953).
17. Topalian, S.L. et al. Safety, activity, and immune correlates of anti-PD-1 antibody in cancer. *N Engl J Med* **366**, 2443-2454 (2012).
18. June, C.H., O'Connor, R.S., Kawalekar, O.U., Ghassemi, S. & Milone, M.C. CAR T cell immunotherapy for human cancer. *Science* **359**, 1361-1365 (2018).
19. Paavonen, J. et al. Efficacy of a prophylactic adjuvanted bivalent L1 virus-like-particle vaccine against infection with human papillomavirus types 16 and 18 in young women: an interim analysis of a phase III double-blind, randomised controlled trial. *Lancet* **369**, 2161-2170 (2007).
20. Darvin, P., Toor, S.M., Sasidharan Nair, V. & Elkord, E. Immune checkpoint inhibitors: recent progress and potential biomarkers. *Exp Mol Med* **50**, 1-11 (2018).
21. Suzuki, M. et al. Boron neutron capture therapy outcomes for advanced or recurrent head and neck cancer. *J Radiat Res* **55**, 146-153 (2014).
22. Moss, R.L. Critical review, with an optimistic outlook, on Boron Neutron Capture Therapy (BNCT). *Appl Radiat Isot* **88**, 2-11 (2014).
23. Luderer, M.J., de la Puente, P. & Azab, A.K. Advancements in Tumor Targeting Strategies for Boron Neutron Capture Therapy. *Pharm Res* **32**, 2824-2836 (2015).
24. Soloway, A.H., Barth, R.F., Gahbauer, R.A., Blue, T.E. & Goodman, J.H. The rationale and requirements for the development of boron neutron capture therapy of brain tumors. *J Neurooncol* **33**, 9-18 (1997).
25. GL, L. Biological effects and therapeutic possibilities of neutrons. *Am J Roentgenol Radium Ther* **36**, 1-13 (1937).
26. Farr, L.E., Sweet, W.H., Locksley, H.B. & Robertson, J.S. Neutron capture

therapy of gliomas using boron. *Trans Am Neurol Assoc* **13**, 110-113 (1954).

27. Hatanaka, H. Clinical results of boron neutron capture therapy. *Basic Life Sci* **54**, 15-21 (1990).
28. Mishima, Y. et al. First human clinical trial of melanoma neutron capture. Diagnosis and therapy. *Strahlenther Onkol* **165**, 251-254 (1989).
29. Soloway, A.H., Hatanaka, H. & Davis, M.A. Penetration of brain and brain tumor. VII. Tumor-binding sulfhydryl boron compounds. *J Med Chem* **10**, 714-717 (1967).
30. Detta, A. & Cruickshank, G.S. L-amino acid transporter-1 and boronophenylalanine-based boron neutron capture therapy of human brain tumors. *Cancer Res* **69**, 2126-2132 (2009).
31. Wongthai, P. et al. Boronophenylalanine, a boron delivery agent for boron neutron capture therapy, is transported by ATB0,+, LAT1 and LAT2. *Cancer Sci* **106**, 279-286 (2015).
32. Hiratsuka, J., Yoshino, K., Kondoh, H., Imajo, Y. & Mishima, Y. Biodistribution of boron concentration on melanoma-bearing hamsters after administration of p-, m-, o-boronophenylalanine. *Jpn J Cancer Res* **91**, 446-450 (2000).
33. Kondo, N., Hirano, F. & Temma, T. Evaluation of 3-Borono-l-Phenylalanine as a Water-Soluble Boron Neutron Capture Therapy Agent. *Pharmaceutics* **14** (2022).
34. Havu-Aurén, K. et al. Uptake of 4-borono-2- <SUP>18</SUP>F fluoro-L-phenylalanine in sporadic and neurofibromatosis 2-related schwannoma and meningioma studied with PET. *European Journal of Nuclear Medicine and Molecular Imaging* **34**, 87-94 (2007).
35. Hsieh, C.H. et al. Evaluation of pharmacokinetics of 4-borono-2-<SUP>18</SUP>F-fluoro-L-phenylalanine for boron neutron capture therapy in a glioma-bearing rat model with hyperosmolar blood-brain barrier disruption. *Journal of Nuclear Medicine* **46**, 1858-1865 (2005).
36. Wang, H.E. et al. Evaluation of 4-borono-2-<SUP>18</SUP>F-fluoro-L-phenylalanine-fructose as a probe for boron neutron capture therapy in a glioma-bearing rat model. *Journal of Nuclear Medicine* **45**, 302-308 (2004).
37. Watanabe, T. et al. Comparison of the pharmacokinetics between L-BPA and L-FBPA using the same administration dose and protocol: a validation study for the theranostic approach using [(18)F]-L-FBPA positron emission tomography in

boron neutron capture therapy. *BMC Cancer* **16**, 859 (2016).

38. Mori, Y., Suzuki, A., Yoshino, K. & Kakihana, H. Complex formation of p-boronophenylalanine with some monosaccharides. *Pigment Cell Res* **2**, 273-277 (1989).
39. Kanno, H. et al. Designation Products: Boron Neutron Capture Therapy for Head and Neck Carcinoma. *Oncologist* **26**, e1250-e1255 (2021).
40. Wittig, A., Sauerwein, W.A. & Coderre, J.A. Mechanisms of transport of p-borono-phenylalanine through the cell membrane in vitro. *Radiat Res* **153**, 173-180 (2000).
41. Porra, L. et al. Accelerator-based boron neutron capture therapy facility at the Helsinki University Hospital. *Acta Oncol* **61**, 269-273 (2022).
42. Nomoto, T. et al. Poly(vinyl alcohol) boosting therapeutic potential of p-boronophenylalanine in neutron capture therapy by modulating metabolism. *Science Advances* **6** (2020).
43. A clinician's perspective on boron neutron capture therapy: promising advances, ongoing trials, and future outlook.
44. Corporation, S.P. (2024).
45. Cheng, X., Li, F.F. & Liang, L.Z. Boron Neutron Capture Therapy: Clinical Application and Research Progress. *Current Oncology* **29**, 7868-7886 (2022).
46. Suzuki, M. et al. A novel concept of treatment of diffuse or multiple pleural tumors by boron neutron capture therapy (BNCT). *Radiother Oncol* **88**, 192-195 (2008).
47. Farías, R.O., Bortolussi, S., Menéndez, P.R. & González, S.J. Exploring Boron Neutron Capture Therapy for non-small cell lung cancer. *Phys Med* **30**, 888-897 (2014).
48. Stinchcombe, T.E. & Bradley, J.D. Thoracic Oncology: Current Standard Therapy and Future Developments. *Journal of Clinical Oncology* **40**, 527-+ (2022).
49. Chang, J.Y. Stereotactic ablative radiotherapy: aim for a cure of cancer. *Ann Transl Med* **3**, 12 (2015).
50. Arroyo-Hernandez, M. et al. Radiation-induced lung injury: current evidence. *BMC Pulm Med* **21**, 9 (2021).
51. Koay, E.J., Owen, D. & Das, P. Radiation-Induced Liver Disease and Modern Radiotherapy. *Semin Radiat Oncol* **28**, 321-331 (2018).
52. Park, H.J. et al. Effects of Radiation Dose on Liver After Free-breathing

Volumetric Modulated Arc Therapy for Breast Cancer. *In Vivo* **36**, 1937-1943 (2022).

53. Raymakers, L. et al. The Effect of Radiation Treatment of Solid Tumors on Neutrophil Infiltration and Function: A Systematic Review. *Int J Radiat Oncol Biol Phys* **120**, 845-861 (2024).
54. Cabral, H. et al. Accumulation of sub-100 nm polymeric micelles in poorly permeable tumours depends on size. *Nat Nanotechnol* **6**, 815-823 (2011).
55. Tabata, Y., Murakami, Y. & Ikada, Y. Tumor accumulation of poly(vinyl alcohol) of different sizes after intravenous injection. *J Control Release* **50**, 123-133 (1998).
56. Otani, R. et al. The Anti-Tumor Effect of the Newly Developed LAT1 Inhibitor JPH203 in Colorectal Carcinoma, According to a Comprehensive Analysis. *Cancers (Basel)* **15** (2023).
57. Rooman, I. et al. Amino acid transporters expression in acinar cells is changed during acute pancreatitis. *Pancreatology* **13**, 475-485 (2013).
58. Harpaz, D. et al. Dissolvable Polyvinyl-Alcohol Film, a Time-Barrier to Modulate Sample Flow in a 3D-Printed Holder for Capillary Flow Paper Diagnostics. *Materials (Basel)* **12** (2019).
59. Seeliger, E., Lenhard, D.C. & Persson, P.B. Contrast media viscosity versus osmolality in kidney injury: lessons from animal studies. *Biomed Res Int* **2014**, 358136 (2014).
60. Wang, X., Yucel, T., Lu, Q., Hu, X. & Kaplan, D.L. Silk nanospheres and microspheres from silk/pva blend films for drug delivery. *Biomaterials* **31**, 1025-1035 (2010).
61. Ye, M., Mohanty, P. & Ghosh, G. Morphology and properties of poly vinyl alcohol (PVA) scaffolds: impact of process variables. *Mater Sci Eng C Mater Biol Appl* **42**, 289-294 (2014).
62. Zhao, H. et al. Multiscale engineered artificial tooth enamel. *Science* **375**, 551-556 (2022).
63. Roome, N.W., Ruttle, L., Williams, L. & Smith, W. The Polyvinyl Alcohols as Blood Substitutes. *Can Med Assoc J* **51**, 293-299 (1944).
64. Himawan, A. et al. Formulation and evaluation of PVA-based composite hydrogels: physicochemical, leachables, and in vitro immunogenicity studies. *J Mater Chem B* (2025).

65. Hattori, Y. et al. Proposal of recommended experimental protocols for in vitro and in vivo evaluation methods of boron agents for neutron capture therapy. *J Radiat Res* **64**, 859-869 (2023).
66. ステラファーマ株式会社 (2023).
67. Mordant, P. et al. Bioluminescent orthotopic mouse models of human localized non-small cell lung cancer: feasibility and identification of circulating tumour cells. *PLoS One* **6**, e26073 (2011).
68. Liang, T.L. et al. A method establishment and comparison of in vivo lung cancer model development platforms for evaluation of tumour metabolism and pharmaceutical efficacy. *Phytomedicine* **96**, 153831 (2022).
69. Gan, W. et al. Establishment of an orthotopic model of lung cancer by transthoracic lung puncture using tumor fragments. *J Thorac Dis* **15**, 2012-2021 (2023).
70. Robinson, B.W., Musk, A.W. & Lake, R.A. Malignant mesothelioma. *Lancet* **366**, 397-408 (2005).
71. Van Gerwen, M. et al. Prognostic factors of survival in patients with malignant pleural mesothelioma: an analysis of the National Cancer Database. *Carcinogenesis* **40**, 529-536 (2019).
72. Ziółkowska, B., Cybulska-Stopa, B., Papantoniou, D. & Suwiński, R. Systemic treatment in patients with malignant pleural mesothelioma - real life experience. *BMC Cancer* **22**, 432 (2022).
73. Suzuki, M. et al. A preliminary experimental study of boron neutron capture therapy for malignant tumors spreading in thoracic cavity. *Jpn J Clin Oncol* **37**, 245-249 (2007).
74. Agency（PMDA）, P.a.M.D. (2021).
75. Peters, S. et al. First-line nivolumab plus ipilimumab versus chemotherapy in patients with unresectable malignant pleural mesothelioma: 3-year outcomes from CheckMate 743. *Ann Oncol* **33**, 488-499 (2022).
76. Shiravand, Y. et al. Immune Checkpoint Inhibitors in Cancer Therapy. *Curr Oncol* **29**, 3044-3060 (2022).
77. Borea, F. et al. Target Therapy in Malignant Pleural Mesothelioma: Hope or Mirage? *Int J Mol Sci* **24** (2023).
78. Aihara, T. et al. BNCT for advanced or recurrent head and neck cancer. *Appl*

*Radiat Isot* **88**, 12-15 (2014).

79. Kato, T. et al. Design and construction of an accelerator-based boron neutron capture therapy (AB-BNCT) facility with multiple treatment rooms at the Southern Tohoku BNCT Research Center. *Appl Radiat Isot* **156**, 108961 (2020).
80. Suzuki, S. et al. Initial evaluation of accelerator-based neutron source system at the Shonan Kamakura General Hospital. *Appl Radiat Isot* **199**, 110898 (2023).
81. Coderre, J.A. et al. Selective targeting of boronophenylalanine to melanoma in BALB/c mice for neutron capture therapy. *Cancer Res* **47**, 6377-6383 (1987).
82. Coderre, J.A. et al. Selective delivery of boron by the melanin precursor analogue p-boronophenylalanine to tumors other than melanoma. *Cancer Res* **50**, 138-141 (1990).
83. Pineda, M. et al. Identification of a membrane protein, LAT-2, that Co-expresses with 4F2 heavy chain, an L-type amino acid transport activity with broad specificity for small and large zwitterionic amino acids. *J Biol Chem* **274**, 19738-19744 (1999).
84. Sloan, J.L. & Mager, S. Cloning and functional expression of a human Na<SUP>+</SUP> and Cl<SUP>-</SUP>-dependent neutral and cationic amino acid transporter B<SUP>0+</SUP>. *Journal of Biological Chemistry* **274**, 23740-23745 (1999).
85. Fukuda, H. et al. Boron neutron capture therapy of malignant melanoma using 10B-paraboronophenylalanine with special reference to evaluation of radiation dose and damage to the normal skin. *Radiat Res* **138**, 435-442 (1994).
86. Segawa, H. et al. Identification and functional characterization of a Na+-independent neutral amino acid transporter with broad substrate selectivity. *J Biol Chem* **274**, 19745-19751 (1999).
87. Yanagida, O. et al. Human L-type amino acid transporter 1 (LAT1): characterization of function and expression in tumor cell lines. *Biochim Biophys Acta* **1514**, 291-302 (2001).
88. Hirai, N. et al. Evaluation of D-isomer of (18)F-FBPA for oncology PET focusing on the differentiation of glioma and inflammation. *Asia Ocean J Nucl Med Biol* **8**, 102-108 (2020).
89. Wang, Z. et al. Tyrosine modified irinotecan-loaded liposomes capable of simultaneously targeting LAT1 and ATB(0,+) for efficient tumor therapy. *J*

*Control Release* **316**, 22-33 (2019).

90. Yamada, N. et al. Engineering Tumour Cell-Binding Synthetic Polymers with Sensing Dense Transporters Associated with Aberrant Glutamine Metabolism. *Sci Rep* **7**, 6077 (2017).
91. Honda, Y. et al. Systemically Applicable Glutamine-Functionalized Polymer Exerting Multivalent Interaction with Tumors Overexpressing ASCT2. *ACS Appl Bio Mater* **4**, 7402-7407 (2021).
92. Guo, H. et al. Polymeric ligands comprising sulfur-containing amino acids for targeting tumor-associated amino acid transporters. *Biomaterials* **293**, 121987 (2023).
93. Yun, D.W. et al. JPH203, an L-type amino acid transporter 1-selective compound, induces apoptosis of YD-38 human oral cancer cells. *J Pharmacol Sci* **124**, 208-217 (2014).
94. Hattori, Y., Ishimura, M., Ohta, Y., Takenaka, H. & Kirihata, M. Visualization of Boronic Acid Containing Pharmaceuticals in Live Tumor Cells Using a Fluorescent Boronic Acid Sensor. *ACS Sensors* **1**, 1394-1397 (2016).
95. Arzt, M., Seidler, C., Ng, D.Y. & Weil, T. Reversible click reactions with boronic acids to build supramolecular architectures in water. *Chem Asian J* **9**, 1994-2003 (2014).
96. Matsumoto, Y. et al. Vascular bursts enhance permeability of tumour blood vessels and improve nanoparticle delivery. *Nat Nanotechnol* **11**, 533-538 (2016).
97. Sun, T., Han, D., Riehemann, K., Chi, L. & Fuchs, H. Stereospecific interaction between immune cells and chiral surfaces. *J Am Chem Soc* **129**, 1496-1497 (2007).
98. Wang, X. et al. Stereochemistry triggered differential cell behaviours on chiral polymer surfaces. *Soft Matter* **6** (2010).
99. Wang, X., Gan, H. & Sun, T. Chiral Design for Polymeric Biointerface: The Influence of Surface Chirality on Protein Adsorption. *Advanced Functional Materials* **21**, 3276-3281 (2011).
100. Zhang, M., Qing, G. & Sun, T. Chiral biointerface materials. *Chem Soc Rev* **41**, 1972-1984 (2012).
101. Ishigami, T., Suga, K. & Umakoshi, H. Chiral Recognition of L-Amino Acids on Liposomes Prepared with L-Phospholipid. *ACS Appl Mater Interfaces* **7**, 21065-21072 (2015).

102. Hu, J., Cochrane, W.G., Jones, A.X., Blackmond, D.G. & Paegel, B.M. Chiral lipid bilayers are enantioselectively permeable. *Nat Chem* **13**, 786-791 (2021).
103. Genchi, G. An overview on D-amino acids. *Amino Acids* **49**, 1521-1533 (2017).
104. Du, S., Wey, M. & Armstrong, D.W. d-Amino acids in biological systems. *Chirality* **35**, 508-534 (2023).
105. Sahoo, S.K., Panyam, J., Prabha, S. & Labhasetwar, V. Residual polyvinyl alcohol associated with poly (D,L-lactide-co-glycolide) nanoparticles affects their physical properties and cellular uptake. *J Control Release* **82**, 105-114 (2002).
106. Wilkinson, A.C. et al. Author Correction: Long-term ex vivo haematopoietic-stem-cell expansion allows nonconditioned transplantation. *Nature* **571**, E12 (2019).
107. Tokura, D. et al. Active control of pharmacokinetics using light-responsive polymer-drug conjugates for boron neutron capture therapy. *J Control Release* **371**, 445-454 (2024).
108. He, H. et al. The basis and advances in clinical application of boron neutron capture therapy. *Radiat Oncol* **16**, 216 (2021).
109. 医薬品医療機器総合機構 医薬品インタビューフォーム_ステボロニン®点滴静注バッグ 9000 mg/300 mL. (2023).
110. Yamaoka, T., Tabata, Y. & Ikada, Y. Comparison of body distribution of poly(vinyl alcohol) with other water-soluble polymers after intravenous administration. *J Pharm Pharmacol* **47**, 479-486 (1995).
111. New, M. & Keith, R. Early Detection and Chemoprevention of Lung Cancer. *F1000Res* **7**, 61 (2018).
112. Trivillin, V.A. et al. Abscopal effect of boron neutron capture therapy (BNCT): proof of principle in an experimental model of colon cancer. *Radiation and Environmental Biophysics* **56**, 365-375 (2017).
113. Khan, A.A., Maitz, C., Quanyu, C. & Hawthorne, F. BNCT induced immunomodulatory effects contribute to mammary tumor inhibition. *PLoS One* **14**, e0222022 (2019).
114. Benitez, D.N.F. et al. Therapeutic Efficacy, Radiotoxicity and Abscopal Effect of BNCT at the RA-3 Nuclear Reactor Employing Oligo-Fucoidan and Glutamine as Adjuvants in an Ectopic Colon Cancer Model in Rats. *Life-Basel* **13** (2023).
115. Shi, Q.Q. et al. Anti-hepatitis, antioxidant activities and bioactive compounds of

Dracocephalum heterophyllum extracts. *Bot Stud* **57**, 16 (2016).

116. Irion, C.I. et al. Col4a3(-/-) Mice on Balb/C Background Have Less Severe Cardiorespiratory Phenotype and SGLT2 Over-Expression Compared to 129x1/SvJ and C57Bl/6 Backgrounds. *Int J Mol Sci* **23** (2022).

# ACHIEVEMENT

1. Original paper
   1. Kakeru Konarita, Kaito Kanamori, Minoru Suzuki, Daiki Tokura, Shota Tanaka, Yuto Honda, Nobuhiro Nishiyama, Takahiro Nomoto. “Poly(vinyl alcohol) potentiating an inert D-amino acid-based drug for boron neutron capture therapy” ***Journal of Controlled Release*** 2024, 37 (10), 385-396.

2. Academic conference oral presentation
   i. International conference
      - K. Konarita, T. Nomoto, K. Kanamori, M. Suzuki, M. Matsui,Y. Miura, N. Nishiyama, “Improvement of therapeutic effect of D-4-boronophenylalanine
      - by poly(vinyl alcohol)” 20th International Congress on Neutron Capture Therapy, Krakow, Poland, June 23th - June 28th, 2024
      - Kakeru Konarita, Daiki Tokura, Minoru Suzuki, Yuto Honda, Nobuhiro Nishiyama, Takahiro Nomoto. “Poly(vinyl alcohol) enhancing therapeutic potential of D-amino acid-based boron drugs for neutron capture therapy”
      - Japan drug delivery system of society Tsukuba, Japan, July 9-11th

   ii. Domestic conference
      - Kakeru Konarita, Takahiro Nomoto, Kaito Kanamori, Minoru Suzuki, Makoto Matsui, Yutaka Miura, Nobuhiro Nishiyama. “Poly(vinyl alcohol)に よる D-4-boronophenylalanine の治療向上”, 17th Japanese Neutron Capture Therapy Society Academic Conference, 2021. July, Best presenter award. Peer-reviewed.
      - Takahiro Nomoto, Yukiya Inoue, Ying Yao, Minoru Suzuki, Kaito Kanamori, Kakeru Konarita, Hiroyasu Takemoto, Makoto Matsui, Nobuhiro Nishiyama, “Development of functional polymers to boost therapeutic potential of boronophenylalanine in neutron capture therapy”, 69th Polymer Symposium、Online. 2020. September, Peer-reviewed.
      - Takahiro Nomoto, Yukiya Inoue, Yao Ying, Kaito Kanamori, Minoru Suzuki, Kakeru Konarita, Makoto Matsui, Nobuhiro Nishiyama. “側鎖に

糖構造を有する高分子とボロノフェニルアラニンから構成される薬物送達システムの設計”, 17th Japanese Neutron Capture Therapy Society Academic Conference, Online, 2021.July, Peer-reviewed

- Kakeru Konarita, Daiki Tokura, Kaito Kanamori, Minoru Suzuki, Yuto Honda, Nobuhiro Nishiyama, Takahiro Nomoto “D-4-boronophenylalnanine と poly(vinyl) alcohol から構成されるホウ素送達システムの検討” 19th Japanese Neutron Capture Therapy Society Academic Conference, Peer-reviewed 2023.7.14-15.
- Takahiro Nomoto, Kakeru Konarita, Minoru Suzuki, Makoto Matsui, Nobuhiro Nishiyama. “ポリビニルアルコールを利用したボロノフェニルアラニンの中性子捕捉療法における治療効果向上”. 37th Japan Drug Delivery Society Academic Conference, Peer-reviewed
- Kakeru Konarita, Daiki Tokura, Minoru Suzuki, Nobuhiro Nishiyama, Takahiro Nomoto. “ポリビニルアルコールによる中性子捕捉療法用 D-アミノ酸ホウ素薬剤の治療効果向上” The 144th Annual Meeting of Pharmaceutical Society of Japan 2024. March. Peer-reviewed

3. Academic conference poster presentation

iii. International conference

- K. Konarita, T. Nomoto, K. Kanamori, M. Suzuki, M. Matsui,Y. Miura, N. Nishiyama, “Improvement of therapeutic effect of D-4-boronophenylalanine by poly(vinyl alcohol)” 19th International Congress on Neutron Capture Therapy, Granada, Spain, September 27th - October 1th, 2021

iv. Domestic conference

- Kakeru Konarita, Takahiro Nomoto, Kaito Kanamori, Minoru Suzuki, Makoto Matsui, Yutaka Miura, Nobuhiro Nishiyama. “Poly(vinyl alcohol) と D-4-boronophenylalanine から構成される薬物送達システムによるホウ素中性子捕捉療法の検討”, 70th Annual Polymer Conference, Online, 2021. May. Peer-reviewed.

4. Others

- Japan Society for the Promotion of Science Special Research Fellow(DC2)

# ACKNOWLEDGEMENT

First and foremost, I would like to extend my heartfelt gratitude to Prof. Nobuhiro Nishiyama for his invaluable discussions, insightful suggestions, and for guiding me toward the doctoral program after I began working. His advice has been both inspiring and motivating, leaving a profound impact on my academic journey.

I am deeply thankful to Prof. Yutaka Miura, Prof. Hiroyuki Nakamura , Prof. Tetsuya Kadonosono, Prof. Katsunori Tanaka and Prof. Masato Sone for their thorough review of this thesis. Their insightful feedback and detailed comments significantly contributed to its improvement.

I would also like to express my appreciation to the members of the Nishiyama Laboratory. My sincere thanks go to Prof. Yutaka Miura for his thought-provoking discussions and for providing numerous opportunities to broaden my perspectives; Dr. Hiroyasu Takemoto for his insightful discussions about polymer science; and Dr. Makoto Matsui for his support in biological experiments and valuable advice.

In particular, I am deeply grateful to Dr. Takahiro Nomoto, who has been my mentor, for his daily discussions, critical insights, and guidance in honing my writing skills. His exceptional support and encouragement greatly facilitated my research.

I also wish to thank my colleagues in the Nishiyama Laboratory, including Dr. Aziz Awaad, Dr. Kaori Taniwaki, Ms. Megumi Sunahara, and Mr. Haochen Guo, for their collaboration, assistance in experiments, and enriching discussions.

I extend my gratitude to Dr. Yuki Mochida, at the Innovation Center of NanoMedicine for their support.

A special thanks to Mr. Kaito Kanamori, Ms. Kana Komoto, whose daily discussions, mutual encouragement, and foundational contributions greatly influenced my research

during my bachelor’s and master’s course.

I am particularly thankful to Mr. Daiki Tokura for his late-night discussions and invaluable advice on both research and life as a researcher.

I also express my gratitude to my colleagues in Nomoto Laboratory, Especially, I thank Mr. Jiang Hanqing for his contributions to the discussions, and Mr. Shota Tanaka for checking the notation of this thesis.

This work was supported by Grant-in-Aid from the Japan Society for the Promotion of Science (JSPS, DC2).

I extend my gratitude to Dr. Yoshinori Sakurai, Dr. Hiroki Tanaka, and Dr. Takushi Takata from Kyoto University for their support with neutron irradiation.

I am also grateful to Mr. Koki Uehara, Mr. Hideki Nakashima, Ms. Yuko Ishino, and Ms. Aya Sudani of Stella Pharma Corporation for their valuable discussions on the physicochemical properties of L-/D-BPA, assistance with the antitumor study, and provision of L-/D-BPA. Additionally, my appreciation also goes to Japan Vam & Poval Co., Ltd. for supplying PVA and sharing relevant information.

Lastly, I would like to express my deepest gratitude to my parents for their unwavering support and encouragement.